

**ASYMMETRIC DIVISION OF DAMAGED PROTEINS IN
PROLIFERATING CELLS**

by

Mary Rose Bufalino

A thesis submitted in conformity with the requirements
for the degree of Doctor of Philosophy
Graduate Department of Medical Biophysics
University of Toronto

© Copyright by Mary Rose Bufalino 2014

ASYMMETRIC DIVISION OF DAMAGED PROTEINS IN PROLIFERATING CELLS

Mary Rose Bufalino
Ph.D., Department of Medical Biophysics
University of Toronto
2014

Abstract

This thesis explores the unequal partitioning of damaged proteins during mitosis and its implications for cell fate. Initially described in unicellular organisms, it was unclear if this method was used *in vivo* in multicellular organisms and had functional consequences in mammalian cells. To determine if this asymmetry was conserved in multicellular organisms, I studied three stem/progenitor populations in *Drosophila*: the larval neuroblast, adult female germline stem cell, and adult intestinal stem cell. Each cell type was found to asymmetrically segregate damaged proteins identified by the 2,4-hydroxynonenal (HNE) modification, which are associated with oxidative stress and age. Both the larval neuroblast and female germline stem cell were found to retain damaged proteins during division, whereas the intestinal stem cell segregated damaged proteins to differentiating progeny. I suggest that functional lifespan, and not cell type, determines the cell that receives the majority of damaged proteins during division. In each cell type, damaged proteins were associated with DE-Cadherin, a common component of the stem cell niche and removal from the niche was associated with reduced damaged protein polarization. Interestingly, when larval neuroblasts were mechanically dissociated from their niche and placed in culture, the internal polarization of damaged proteins was found to increase with progression through the cell-cycle. Therefore, I suggest that both the

niche and intrinsic factors play a role in the asymmetric division of damaged proteins. To determine if an asymmetric division of damaged proteins influenced cell fate, I used a mammalian cell line with inducible expression of misfolded Huntingtin, which shares similar properties to damaged proteins. This study also revealed that the conformation of damaged proteins impacts cell fate: cells with diffuse Huntingtin displayed greater proliferation and reduced resistance to stress. Tracking cells containing an aggregate with live-imaging revealed that the cell that inherits the aggregate has a longer cell-cycle and an enhanced capacity to differentiate. Therefore, the asymmetric inheritance of damaged proteins impacts cell fate. In the final chapter of this thesis, I discuss the implications of an asymmetric division of damaged proteins on cell fate and how this information can be applied to cancer treatments.

Acknowledgements

I was very fortunate to have the support of many individuals while pursuing a Ph.D. Foremost I would like to thank my supervisor, Derek van der Kooy, who gave me the flexibility and support to pursue my interests, which were often quite different from the research programs in the lab. With his keen interest in diverse fields, he was always prepared to discuss my varied ideas for new projects. I would also like to thank my committee members, Gabrielle Bouliane and Gordon Keller, for their support and guidance, which has enabled me to complete my Ph.D.

Working on the 11th floor of the Terrance Donnelly Centre for Cellular and Biomolecular Research has given me the opportunity to work alongside members of the Zandstra and Audet lab in addition to the van der Kooy lab. This wonderful mix of people meant that at any time, day or night, there was always someone to help fix a piece of equipment, discuss scientific theories and provide comedic relief. I am particularly indebted to Susan Runciman and Brenda Coles who were always willing to lend a helping hand.

Many people directly contributed to this research. Ulrich Tepass and Benjamin Ohlstein generously shared fly stocks, Volker Hartenstein kindly provided an antibody, Leslie Thompson shared her cancer cell line, and Jason Moffat shared his Incucyte live-imaging system. Pier-Andree Penttila, the flow cytometry technician in the Donnelly Centre, provided her sorting expertise and time to optimize the cancer cell sorting protocol on many nights.

Of course, this work would not have been possible without the support of my family and friends. Thank you.

Table of Contents

Abstract	ii
Acknowledgements	iv
Table of Contents	v
List of Figures	viii
List of Abbreviations	ix
<u>Chapter 1: General Introduction</u>	1
The relationship between reactive oxygen species and age	2
Mechanisms that protect cells from the negative consequences of ROS	4
Example of a degradation resistant protein modification: 2,4 hydroxynonenal	5
Asymmetric division	6
Asymmetric division of damaged proteins	9
Stem/progenitor populations in Drosophila	10
<i>Germline stem cell</i>	<i>10</i>
<i>Neuroblast</i>	<i>12</i>
<i>Intestinal stem cell</i>	<i>13</i>
A model for studying cell fate after asymmetric division: Cancer cells	14
Roles of ROS in Cancer	15
Asymmetric division of cancer cells	16
PC12 cells are a cancer cell line used as a model for neural differentiation	18
Theories on huntingtin aggregation and toxicity	19
Htt provides a model of damaged proteins	20
Research goals	21
<i>Specific aims and hypotheses</i>	<i>21</i>
<u>Chapter 2: The asymmetric segregation of damaged proteins is stem cell-type</u> dependent	23
Summary	24

Introduction.....	25
Materials and methods	27
<i>Flies</i>	<i>27</i>
<i>Immunohistochemistry.....</i>	<i>28</i>
<i>Neuroblast cell culture</i>	<i>29</i>
<i>Image analysis</i>	<i>30</i>
<i>Statistical analysis</i>	<i>30</i>
Results and discussion	31
<i>HNE is a marker of damaged proteins that accumulate with oxidative stress and age</i>	<i>31</i>
<i>Stem cells and progeny differ in HNE levels</i>	<i>35</i>
<i>Intracellular HNE distributes asymmetrically.....</i>	<i>36</i>
<i>In each stem cell population HNE associates with a niche adhesion molecule</i>	<i>40</i>
<i>GSCs displaced from their niche lose some but not all HNE polarization</i>	<i>43</i>
<i>The extent of DCAD polarization predicts HNE asymmetry in ISCs</i>	<i>44</i>
<i>Both niche-dependent and -independent factors are responsible for HNE polarization in NBs</i>	<i>44</i>
<i>Conclusions.....</i>	<i>46</i>
<u>Chapter 3: The aggregation and inheritance of damaged proteins determines cell fate during mitosis</u>	57
Summary	Error! Bookmark not defined.
Introduction.....	59
Materials and methods	61
<i>Cell culture</i>	<i>61</i>
<i>Cell sorting</i>	<i>62</i>
<i>Aggregate induction.....</i>	<i>62</i>
<i>PrestoBlue assay.....</i>	<i>62</i>
<i>Cell proliferation</i>	<i>63</i>

<i>Immunocytochemistry</i>	63
<i>Stress exposure</i>	64
<i>Live-imaging</i>	64
<i>Statistics</i>	65
Results and discussion	65
<i>Cells containing an inclusion body have a longer cell-cycle than cells containing diffuse Htt</i>	65
<i>Cells containing an inclusion body are more resistant to stress than cells with diffuse Htt</i>	70
<i>Live-imaging reveals asymmetric inheritance of inclusion bodies impacts cell fate</i>	73
<i>Conclusions</i>	76
<u>Chapter 4: General Discussion</u>	79
Functional significance of asymmetric damaged protein inheritance in vivo	80
Potential mechanisms of damaged protein polarization	82
Advantages of asymmetric damaged protein division	84
Cancer treatments that induce protein aggregation	87
Theories on the role of inclusion bodies in cell fate decisions	88
Conclusions	90
<u>Reference List</u>	91

List of Figures

Figure 1: GSCs accumulate more HNE with age compared to ISCs, indicating separate modes of HNE distribution during mitosis.....	33
Figure 2: HNE is asymmetrically distributed in the GSC, NB, and ISC	38
Figure 3: DCAD and HNE co-localize	41
Figure 4: The niche is involved in HNE asymmetry	47
Figure 5: Damaged proteins in the GSC, ISC and NB	50
Figure 6: HNE localization measurements in the mitotic GSC, NB, and ISC	53
Figure 7: Localization of HNE in GSCs and ISCs removed from the stem cell niche	55
Figure 8: Inclusion body containing cells have a longer cell cycle than diffuse cells	68
Figure 9: Increasing the number of inclusion body containing cells by inhibiting palmitoylation increases resistance to stress	71
Figure 10: Live-imaging reveals differences in cell-fate of asymmetrically dividing inclusion body cell progeny	77

List of Abbreviations

2-BP	2-bromopalmitate
ANOVA	Analysis of variance
BMP	Bone morphogenetic protein
CB	Cystoblast
DCAD	DE-Cadherin
EB	Enteroblast
EC	Enterocyte
EE	Enteroendocrine cell
FACS	Fluorescence activated cell sorting
GFP	Green fluorescent protein
GMC	Ganglion mother cell
GSC	Germline stem cell
HNE	2,4-hydroxynonenal
Htt	Huntingtin
ISC	Intestinal stem cell
NB	Neuroblast
PBS	Phosphate buffered saline
Raps	Rapsynoid
ROS	Reactive oxygen species
UP	Ubiquitinated proteins

CHAPTER 1

General Introduction

All cells respond differently to stress. Some become quiescent, while others proliferate, differentiate or die. These responses may depend on cell type and/or environment, which influence processes such as the sequestering of stress by-products and ultimately determine cell fate. Understanding how these processes are regulated in proliferating cells, such as stem cells and cancer cells, is essential for revealing mechanisms of aging and novel cancer treatments. Currently, it is unknown how stem cells manage the by-products of stress *in vivo* and how this is linked to cell fate.

Here, I begin by analyzing the distribution of damaged proteins, a by-product of stress linked to aging and disease, in three *Drosophila* cell types that contribute to organs (brain, intestine, and ovary) through proliferation. Next, I describe cell-intrinsic and extrinsic mechanisms that contribute to the proper segregation of damaged proteins in these cells. Finally, I explore how aggregation and inheritance of damaged proteins in proliferating cells, in this case a cancer cell line, impacts cell fate.

The relationship between reactive oxygen species and age

In general, aging describes the decline in function that an organism experiences over time. A recent analysis of the aging literature determined nine characteristics of aging: epigenetic alterations, telomere attrition, genomic instability, altered intercellular communication, stem cell exhaustion, cellular senescence, mitochondrial dysfunction, deregulated nutrient sensing, and loss of proteostasis (Lopez-Otin et al., 2013). It is still unclear how each of these events contributes to aging, as many of them are related. One

similarity between these events is their susceptibility to disruption by reactive oxygen species (ROS).

ROS have been suggested as a cause of aging since 1956 when the *Free Radical Theory of Ageing* was proposed (Harman, 1956), which suggests that aging is caused by an accumulation of molecules damaged by ROS that disrupt normal cell function (Giorgio et al., 2007). ROS are constantly being produced as a by-product of aerobic metabolism, particularly at complex I and III of the electron transport chain where electrons can leak out and transfer to molecular oxygen resulting in the superoxide radical (Finkel et al., 2000). ROS have an unpaired electron, making them strong oxidizing agents that can interact and modify the function of biomolecules including proteins, lipids, and DNA. Since the emergence of this theory, there have been 300+ additional theories that consider ROS and the damage it causes to be a significant part of aging and many studies have supported these theories. For example, studies of long-lived *C. elegans* mutants revealed that their accumulation of damaged molecules with age is reduced compared to wild type (Brys et al., 2007). Furthermore, the increased activity of systems responsible for removing damaged molecules from cells has been found to extend lifespan in yeast (Kruegel et al., 2012).

In adult multi-cellular organisms, stem cells are responsible for the maintenance and regeneration of tissues, as they have the ability to self-renew and produce differentiated cells, which perform the specialized functions of an organ. The number, function, and differentiation capabilities of stem cells have been observed to decline with age *in vivo* (Choi, 2009; Liu and Rando, 2011) and it has been proposed that by slowing the aging of stem/progenitor cells, the effects of aging will be reduced for the whole

organism (Liu and Rando, 2011). The susceptibility of stem cells to aging may explain why they are generally found to have an enhanced system to protect themselves from ROS (Jang & Sharkis, 2007).

Mechanisms that protect cells from the negative consequences of ROS

Multiple mechanisms exist to regulate the levels of ROS and the molecules they modify. For example, highly reactive superoxide anions are converted into water and oxygen by superoxide dismutase, glutathione peroxidase and catalase. Superoxide dismutase catalyzes the reaction of superoxide to hydrogen peroxide, and glutathione peroxidase and catalase catalyze the reaction of hydrogen peroxide to water and oxygen (Giorgio et al., 2007). The importance of these enzymes for resisting the negative effects of ROS has been demonstrated in many organisms. For example, superoxide dismutase mutant *Drosophila* have reduced lifespan and resistance to oxidative stress induced by Paraquat, a xenobiotic that produces superoxide radicals in a NADH-dependent reduction (Phillips et al., 1989). Furthermore, lifespan can be extended when catalase is overexpressed in the mitochondria of mice (Schriner, 2005).

When proteins interact with ROS that escape degradation they become oxidized, which generally disrupts their function (Wong et al., 2010). When a protein is oxidized modifications result such as the formation of disulfide bonds, which can be reversed by enzymes; however, the majority of modifications are irreversible and the protein must be degraded (Grune et al., 2004).

Often damaged proteins are further modified to target them for degradation. For example, proteins can be ubiquitinated targeting them for degradation through the proteasome, lysosome, or autophagosome. Proteins can be modified with a single ubiquitin molecule or a chain of ubiquitin molecules and the location, and length of the ubiquitin chain are hypothesized to mark the protein for degradation through one pathway (Clague and Urbe, 2010). The proteasome consists of the core (20S) and regulatory (19S) units. The core is responsible for proteolytic activity and contains subunits with chymotrypsin-like, trypsin-like and caspase-like activity (Chen et al., 2011). The regulatory unit facilitates this process by recognizing proteins marked for degradation, removing their ubiquitin tag, unfolding the protein and allowing it access to the core (Chen et al., 2011). Many plasma membrane proteins are degraded in lysosomes, a membrane-bound organelle that contains acid hydrolases (Luzio et al., 2007). During autophagy, a double-membrane surrounds the item to be degraded forming an autophagosome, which then fuses with a lysosome to be degraded (Luzio et al., 2007).

Example of a degradation resistant protein modification: 2,4 hydroxynonenal

Despite these safeguards, some damaged proteins are able to persist resulting in an accumulation with age. One example is 2,4 hydroxynonenal (HNE), a product of lipid peroxidation that is highly reactive and readily forms covalent bonds with proteins that have been oxidized, making them resistant to proteolysis through the proteasome, although they are susceptible to lysosomal degradation (Friguet and Szweda, 1997; Marques et al., 2004).

HNE has previously been identified as an indicator of oxidative stress, contains carbonyl groups (a post-translational modification that can affect the catalytic activity of proteins and increases with age), and identifies a wider range of proteins than another indicator of lipid peroxidation, malondialdehyde, and a method to identify carbonylated proteins using dinitrophenyl hydrazone (Toroser et al., 2007). HNE is toxic to neurons, and cells in general, as it can modify and disrupt the function of proteins involved in cell structure, metabolism, stress, and communication (Butterfield et al., 2011). Furthermore, increased levels of lipid peroxidation products are common to many neurodegenerative diseases, including cognitive impairment and Alzheimer's (Butterfield et al., 2011; Markesbery, 1998).

Asymmetric division

Certain cells have an additional method to rid themselves of damaged proteins, similar to HNE, that evade degradation: cell division. If damaged proteins are distributed evenly between two cells during division, each cell will then contain half the load of damaged proteins as the initial cell. As damaged proteins (and other molecules) are diluted, so are their negative effects on the cell. One theory proposes that dilution through cell division is the most effective method for protecting a cell from damaged molecules and therefore aging (Gladyshev, 2012). When a cell dilutes damage through division, it depends less on the use of mechanisms that degrade damaged molecules, such as enzymes. These protective mechanisms also contribute to the level of damage in a cell, as energy is required to create them and in many cases to perform their function;

furthermore, they may release by-products that can be toxic upon accumulation. In complex multi-cellular organisms, frequent divisions of every cell would not allow for the production of specialized cells that require an extended non-mitotic state to perform their function. Alternatively, dividing cells in a multi-cellular organism could protect one cell from aging by asymmetrically segregating damage during mitosis.

In general, a division can be described as asymmetric if it involves the unequal partitioning of intracellular components that result in sister cells with different fates (Horvitz & Herskowitz, 1992). A conserved trait, asymmetric division has been described in both uni-cellular and multi-cellular organisms to segregate components as simple as proteins and as complex as organelles. The strongest evidence of asymmetric division is the finding that proteins polarized during mitosis are essential for the differential cell fates of sister cells. For example, the asymmetric segregation of Numb during division of sensory organ precursor cells in *Drosophila* is required to produce the cellular diversity needed for the development of mechanosensory bristles. Without Numb, mutants are unable to produce normal sensory organs as they lack inner cells required for proper function (Neumuller & Knoblich, 2009).

Asymmetric division is inevitable for unique cellular components that exist in a single copy, such as the mother centrosome. The centrosome is an organelle involved in microtubule-nucleation and mitotic spindle orientation and replicates prior to division to produce a mother and daughter centrosome. The mother centrosome is distinct from the daughter, as it is associated with more microtubules after centrosome duplication (Yamashita et al., 2007). The mother centrosome is also hypothesized to be associated with cell fate determinants. It has been found to preferentially segregate to one cell type

in many model systems during an asymmetric division that results in two distinct cells (Yamashita et al., 2007; Pereira et al., 2001; Januschke et al., 2011; Wang et al., 2009). For example, messenger RNA has been found to localize to the centrosome during interphase, resulting in its asymmetric segregation during mitosis (Lambert & Nagy, 2002).

Histones and DNA also have been found to asymmetrically segregate to one cell type during mitosis. In *Drosophila* male germline stem cells, newly synthesized canonical H3 histones are segregated to the differentiating daughter cell (Tran et al., 2012). In many stem cell models, the template or ancestral chromosome has been observed to segregate to the stem cell during asymmetric division (Karpowicz et al., 2009; Karpowicz et al., 2005; Shinin et al., 2006; Bussard et al., 2010). This has been described as a protective mechanism, based on the immortal strand hypothesis, which suggests it prevents the accumulation of mutations resulting from DNA replication in stem cells (Cairns, 1975). It is possible that not all chromosomes are asymmetrically segregated. For example, nonrandom chromosome segregation was found only for the sex chromosomes in *Drosophila* male germline stem cells (Yadlapalli & Yamashita, 2013). Although the immortal strand hypothesis has been hotly debated since its inception (Lansdorp, 2007), asymmetric division has been demonstrated to protect one cell from aging through the segregation of damaged cellular components.

Asymmetric division of damaged proteins

The asymmetric inheritance of damage was first observed in yeast, where carbonylated proteins are retained by the mother cell during asymmetric division, resulting in a daughter bud cell relatively free of damaged proteins (Aguilaniu et al., 2003). The level of ROS and ability to produce carbonylated proteins in response to stress did not differ between the mother and bud, suggesting that asymmetric segregation and not increased production of damaged proteins led to greater levels of carbonylated proteins in mother cells. Furthermore, in conditions of increased oxidative stress in yeast mutant for ROS scavenging enzymes, asymmetric inheritance of damaged proteins persisted, suggesting that this segregation is important for bud cell fitness (Aguilaniu et al., 2003).

The amount of damaged proteins received during division has been correlated with decreased fitness, measured by a decline in growth rate, in *E. coli* (Lindner et al., 2008). In this study, live imaging was used to track the inheritance of an insoluble protein present in heat-stressed cells that was fused to yellow fluorescent protein. It is interesting to note that these single aggregates were not actively transported to one region of the cell, but simply remained in the region of the cell where they were produced. This allowed the effects of the protein aggregate and the old pole of the cell to be dissociated, revealing that both protein aggregates and old poles are associated with a decreased growth rate (Lindner et al., 2008).

This asymmetric inheritance of damaged proteins during mitosis appears to be a well-conserved phenomenon, and has been observed for proteins marked for degradation

in *Drosophila* blastoderm cells and human embryonic and mammalian fibroblast cell lines (Fuentelba et al., 2008). Furthermore, asymmetric division may contribute to the finding that undifferentiated murine embryonic stem cells and not their differentiated progeny accumulate damaged proteins such as carbonylated proteins and advanced glycation end products; however, the localization of damaged proteins during mitosis was not reported in this study (Hernebring et al., 2006). So far, no reports have described an asymmetric segregation of damaged proteins in adult stem cells *in vivo*. It is also unclear whether this asymmetric division influences cell fate, as a symmetric division resulting in two human embryonic stem cells, identified by positive Oct4 staining, displayed asymmetric segregation of a transcription factor marked for degradation (Fuentelba et al., 2008). Still, it is possible that the cells had different cell fates even though they both stained positive for Oct4, as the behaviour of the cells was not observed.

In summary, previous studies have left three major topics unexplored in multicellular organisms: 1) Existence of asymmetric segregation of damaged proteins *in vivo*; 2) Mechanism(s) of damaged protein segregation; 3) Effect(s) of asymmetric damaged protein inheritance on cell fate. To fill the first two gaps, I focused on stem/progenitor cells *in vivo* and to address cell fate I employed an *in vitro* model.

Stem/progenitor populations in *Drosophila*

Germline stem cell

In female *Drosophila*, eggs are produced by a pair of ovaries each consisting of 12-16 ovarioles. Each ovariole contains a chain of developing egg chambers and a

germarium, the most apical structure where the GSCs are located. GSCs are maintained by the stem cell niche, which consists of terminal filament cells, cap cells, and escort stem cells (Kirilly & Xie, 2007). Adherens junctions dependent on DE-Cadherin and β -catenin are required to anchor GSCs to cap cells and maintain their position in the niche. Without DE-Cadherin or β -catenin expression, all GSCs are lost within 2 weeks (Song et al., 2002). GSCs must remain closely associated with cap cells because bone morphogenetic protein (BMP) is secreted by cap cells and suppresses transcription of a differentiation gene, bag of marbles (Fuller et al., 2007). When bag of marbles expression is lost, the germarium becomes filled with proliferating GSC-like cells (Ohlstein & McKearin, 1997).

Through asymmetric division GSCs self-renew and produce one differentiated cystoblast, which goes through four rounds of division with incomplete cytokinesis to finally generate a 16-cell cyst (Kirilly et al., 2007). This asymmetry appears to be mediated by the niche and not the segregation of intrinsic cell fate determinants (Deng & Ling, 1997; Lu et al., 2012). This is despite the presence of a unique organelle in GSCs, the spectrosome. Each GSC contains a spectrosome, an organelle rich in spectrin that is involved in orientation of the mitotic spindle. During asymmetric division the spectrosome is inherited by the GSC; however, in mutants lacking spectrosomes the misorientation of the mitotic spindle does not prevent GSCs from dividing asymmetrically (Deng & Lin, 1997). Furthermore, the niche is also responsible for creating polarity within GSCs. The small GTPase Rac becomes activated within GSCs only where the GSC is in contact with the niche. This results in orientation of the mitotic

spindle such that one cell will remain within the niche and one cell will be displaced from it, ultimately resulting in cells with different fates (Lu et al., 2012).

Due to the role of the niche in GSC specification and maintenance, it is not surprising that it also effects how GSCs age. Over time, GSCs decline in number and the ability to produce cysts. This decline is enhanced when the level of niche signaling molecules (BMPs) is decreased, demonstrating an effect of the environment on stem cell aging (Pan et al., 2007). It is interesting to note that intrinsic factors are also responsible for GSC aging, as the effects of aging are attenuated when intrinsic levels of ROS are reduced by superoxide dismutase overexpression (Pan et al., 2007).

Neuroblast

Larval NBs are responsible for creating the neurons and glia of the adult brain in *Drosophila*. Most neurons of the adult brain are produced by the approximately 85 NBs in the central brain (Knoblich, 2008). Within the central brain of each hemisphere, the mushroom body houses 4 NBs that are responsible for producing neurons involved in learning and memory. The ventral nerve cord contains 30 NBs per hemisegment that produce the neurons of the thoracic and abdominal ganglia. Both the NBs of the central brain and ventral nerve cord are specified from the ventral neuroectoderm in the embryo (Knoblich, 2008). Signals from surface glia to central brain NBs initiate their mitotic activity in the larval brain and also appear to modulate NB proliferation. When adhesion between surface glia and NBs is disrupted by mutating DE-Cadherin in glia cells, the mitotic activity of NBs is reduced (Dumstrei et al., 2003). In contrast, the optic lobe NBs arise from neuroepithelial cells in the larval brain and they produce neurons involved in visual processing in the adult (Sousa-Nunes et al., 2010).

In general, NBs divide asymmetrically to produce one NB and one ganglion mother cell (GMC), which differ both in cell fate and morphology. GMCs are one-eighth the size of NBs and divide symmetrically to form a pair neurons or glia. The exception to this rule is the Type II NBs, which have been found in the dorsomedial region of the central brain and produce transit amplifying GMCs that can have limited self-renewal capacity allowing them to produce 10 neurons (Bello et al., 2008; Boone et al., 2008).

The asymmetric segregation of proteins in the NB is well documented. The plane of division is established by Bazooka (Par3), Par6, atypical protein kinase C and Pins (Rapsynoid) / Gai complexes, which localize to the cortex of the NB opposite to the site of GMC production (Inaba & Yamashita, 2012). For example, in *Drosophila* with a Pins loss of function mutation the size difference between NBs and GMCs is lost resulting in two cells of a similar size; however, Pins does not alter cell fate as only the GMC-like cell contains nuclear Prospero, a GMC cell fate determinant (Parmentier et al., 2000). In addition to Prospero, the cell fate determinants Numb (associated with Partner of Numb), Miranda, Brat, and Staufen are segregated to the GMC during division (Inaba & Yamashita, 2012). NB division is also asymmetric with respect to centrosome inheritance, the mother centrosome is segregated to the GMC during division (Januschke et al., 2011).

Intestinal stem cell

Approximately 800-1000 ISCs are located throughout the posterior midgut of *Drosophila* attached to the basement membrane through integrin-dependent adhesion (Goulas et al., 2012). Through asymmetric division ISCs self-renew and produce an enteroblast, which can differentiate into an absorptive enterocyte or secretory

enteroendocrine cell and these differentiated cells are replaced approximately every week (Micchelli and Perrimon, 2006; Ohlstein and Spradling, 2006). ISCs and enteroblasts are closely associated through junctions rich in Armadillo, which is a binding partner of DE-Cadherin (Ohlstein and Spradling, 2006). Different levels of Delta/Notch signaling in ISCs and enteroblasts are responsible for the differentiation of enteroblasts into either enterocytes or enteroendocrine cells (Ohlstein and Spradling, 2007). For example, when Notch signaling is reduced in temperature sensitive Notch mutants grown at the non-permissive temperature, clusters of proliferating ISC-like cells are produced at the expense of differentiated cells (Micchelli and Perrimon, 2006).

Recently, asymmetric segregation of proteins was reported in ISCs. Polarity was induced in ISCs in areas that were in contact with the basement membrane through integrins. This resulted in polarization of Par3, Par6, and atypical protein kinase C and their inheritance by the enteroblast (Goulas et al., 2012). Even though the Par complex is well characterized in NBs, the way asymmetric division of the Par complex determines cell fate in ISCs is currently unknown. No effect on ISC division was found in loss-of-function mutants for known NB cell fate determinants (Goulas et al., 2012).

A model for studying cell fate after asymmetric division: Cancer cells

In vivo, cell fate is influenced by many factors. The interaction of stem cells with their niche and the physical displacement of daughter cells outside of the niche make it difficult to determine what role, if any, unequal damaged protein inheritance has on cell fate. *In vitro*, the environment of a cell can be controlled to a greater extent and a single

factor, such as damaged protein inheritance, can be manipulated allowing for the study of its impact on cell fate. Due to their proliferative nature, cancer cells are commonly available as cell lines and they have the advantage of sharing many properties of stem cells.

Similar to stem cells, sub-populations of cancer cells also have the ability to self-renew and differentiate and have been referred to as cancer stem cells and tumor initiating cells (Reya et al., 2001). Cancer stem cells may arise from stem cells or committed progenitors that have acquired mutations that allow for tumor initiation and maintenance (Clarke & Fuller, 2006). Evidence of cancer stem cells has been found in many tumors, including the mouse brain, skin, and intestine (Gilbertson & Graham, 2012). Furthermore, they may also benefit from the asymmetric segregation of damaged proteins, as this would allow a subset of cells to reset their age and potentially increase their resistance to damage inducing chemotherapies.

Roles of ROS in Cancer

Another characteristic shared by stem cells and cancer cells is their wide range of responses to different levels of ROS. In general, cancer cells are reported to have higher levels of ROS than normal cells as a result of enhanced growth (Gupta et al., 2012). These high levels of ROS may promote further proliferation, as ROS are needed for growth factors and receptor tyrosine kinases for cell cycle progression (Gupta et al., 2012). In contrast, many chemotherapeutic and radiotherapeutic agents cause cancer cell lethality by increasing ROS levels (Gupta et al., 2012).

Therefore, cancer cells are still susceptible to the negative consequences of high ROS levels. One strategy to mitigate cytotoxicity is to upregulate enzymes involved in reducing ROS. For example, multi-drug resistant leukemia cells have increased levels of catalase and are less susceptible to hydrogen peroxide exposure (Lenehan et al., 1995). Bladder cancer cells have also been shown to increase levels of an antioxidant, reduced glutathione, concurrently with increasing superoxide dismutase. This increases their resistance to arsenic trioxide, a ROS inducing chemotherapeutic (Hour et al., 2004). These defense mechanisms may be more prevalent in tumor initiating cells, which have been proposed to be responsible for tumor recurrence after treatment (Reya et al., 2001). So far, tumor initiating cells from breast cancer (Diehn et al., 2009; Reya et al., 2001), gastrointestinal cancer (Ishimoto et al., 2011), and glioblastoma (Bao et al., 2006) populations have been reported to possess enhanced defense mechanisms against oxidative stress. ROS that evade these defenses can cause the build up of damaged proteins, such as those modified by the previously discussed HNE, which has been found to reduce proliferation and induce apoptosis in many types of cancer cells (Barrera, 2012). Therefore, a mechanism to eliminate damaged proteins from tumor initiating cells, such as asymmetric division, may contribute to their ability to escape ROS-inducing chemotherapies and lead to tumor recurrence.

Asymmetric division of cancer cells

So far, the asymmetric division of damaged proteins in cancer cells has not been reported; however, cancer cells are capable of asymmetric division. Cells from lung

adenocarcinoma, normal *MYCN* copy number neuroblastoma, glioma, and colon cancer have been found to undergo asymmetric divisions (Pine et al., 2010; Izumi & Kaneko, 2012; Lathia et al., 2011; O'Brien et al., 2012; Bu et al., 2013). CD133, a protein associated with self-renewal, has been found to asymmetrically segregate during division of rare lung adenocarcinoma and glioma cells (Pine et al., 2010; Lathia et al., 2011). Proteins used to mark differentiated cells (Cytokeratins and prosurfactant apoprotein-C) were also found to polarize during mitosis in a small percentage of lung adenocarcinoma cells (Pine et al., 2010). Colon cancer cells also display a polarized distribution of markers for self-renewal (ALDH1) and differentiation (CK20 and Numb) (Bu et al., 2012; O'Brien et al., 2012). These results were interpreted as evidence that asymmetric division in cancer cells result in distinct cell fates; however, cells were not tracked after mitosis to determine if a functional difference existed between the two daughter cells. The same limitation exists in a report describing asymmetric division of normal *MYCN* copy number neuroblastoma cells. Cells were found to divide asymmetrically with respect to NuMA, a protein involved in spindle orientation; however, no experiment addressed the fate of the cells after this asymmetric division (Izumi & Kaneko, 2012).

Single glioma cells tracked using live-imaging revealed that these cells can undergo four type of division: self-renewing symmetric, terminal differentiated symmetric, asymmetric to produce a self-renewing and differentiated cell, and asymmetric that results in one self-renewing cell and one cell that undergoes apoptosis (Lathia et al., 2011). One limitation of this study was its dependence on immunocytochemistry to identify mitotic cells with an unequal distribution of CD133 and differentiated cells. This prevented the authors from asking if the cell that inherits more

CD133 during division retains the property of self-renewal while the cell containing less CD133 differentiates. To determine if cell fate is influenced by the inheritance of a protein it is necessary to track the proteins localization and identify the fate of the cells following division using live-imaging. This can be accomplished using a fluorescently tagged protein and employing a cell line that is capable of producing differentiated cells that have a distinct morphology, such as the PC12 cell line.

PC12 cells are a cancer cell line used as a model for neural differentiation

Originally isolated from a rat tumor (pheochromocytoma) of the adrenal medulla in 1976, PC12 cells are easily propagated in culture, capable of neuronal differentiation, and maintain their tumorigenic potential (Greene & Tischler, 1976). When exposed to nerve growth factor, PC12 cells readily differentiate into cells that resemble sympathetic ganglion neurons and can release dopamine and noradrenaline (Westerink & Ewing, 2008). These neurons are easily identified by their long neurites, which reach ~100 μm in length within 4 d (Das et al., 2004). For this reason they have been widely used as models for neuronal differentiation, neurite outgrowth, exocytosis and disease.

For example, PC12 cells have been used to model Huntington's Disease, by transfecting cells with exons of the *IT15* gene with an abnormal expansion (>40) of CAG repeats (Apostol et al., 2003). In healthy cells the *IT15* gene encodes for huntingtin (Htt), which is involved in many cellular processes including vesicle transport, transcriptional regulation and clathrin-mediated endocytosis (Arrasate & Finkbeiner, 2012). Abnormal CAG repeats result in an abnormal number of glutamine repeats in Htt, disrupting its

normal functions. Interestingly, although abnormal Htt (herein referred to as Htt) is ubiquitously expressed, the brain is the primary site of degeneration where there is substantial depletion of neurons in the striatum and cerebral cortex (Gil & Rego, 2008).

Theories on huntingtin aggregation and toxicity

Currently, the mechanisms of Htt toxicity are still debated (Todd & Lim, 2013). It has been proposed that neurodegeneration is caused both by the loss of function of the wild-type protein and the toxic effects of the misfolded protein (Gil & Rego, 2008). One hypothesis for Htt toxicity is that it depends on the structural conformation of Htt. Htt exists in two structural conformations within the cell: diffuse molecules and aggregates termed inclusion bodies or aggresomes, which consist of insoluble β -pleated sheets (Arrasate & Finkbeiner, 2012). Inclusion bodies are not unique to Huntington's Disease and can occur when proteins are misfolded or modified due to stress. Inclusion bodies are hypothesized to arise either when protein monomers passively move in the cell until they reach and contribute to an inclusion body or when multiple smaller aggregates are actively transported along microtubules to the site of an inclusion body (Kopito, 2000).

Inclusion bodies are a hallmark of Huntington's Disease and initial theories suggested that they were responsible for inducing a diseased state by creating complexes with essential wild-type proteins and disrupting their function (Arrasate et al., 2004). The studies that followed found that inclusion bodies do not predict neuronal death, as their immunohistochemical distribution did not correlate with the areas of the brain or neuronal sub-types that experience the greatest cell death during disease (Gutkunst et al.,

1999; Kuemmerle et al., 1999). Furthermore, inclusion bodies did not predict cell death when individual striatal neurons transfected with Htt-GFP containing 47 CAG repeats were tracked using live-imaging (Arrasate et al., 2004). Live-imaging revealed that one day after transfection, neurons with and without an inclusion body had a similar risk of death. It is interesting to note that the neurons with inclusion bodies were observed to contain higher levels of Htt-GFP after transfection. Since higher levels of Htt-GFP predicted reduced longevity, this finding suggests that inclusion bodies may protect cells from the toxic effects of Htt (Arrasate et al., 2004). Diffuse Htt may cause toxicity by overloading and impairing the function of the proteasome, resulting in the accumulation of other proteins targeted for degradation and cell stress. By sequestering Htt, inclusion bodies may prevent proteasome impairment and cell death (Arrasate et al., 2004).

Htt provides a model of damaged proteins

As both damaged proteins and Htt impair the proteasome and decrease a cell's ability to resist stress, Htt can be used as a model for damaged proteins (Hipp et al., 2012). Furthermore, Htt can be fused with GFP making it amenable to live-imaging. For example, the expression of Htt-GFP has been used to track the asymmetric inheritance of aggregates in human embryonic and mammalian somatic cell lines (Rujano et al., 2006). Cells resulting from asymmetric division were not followed over-time and it is unknown how Htt aggregates influence cell fate. As Huntington's Disease results from neuronal death linked to Htt content, research has focused on the effect of aggregate and diffuse Htt on cells after neural differentiation.

Research goals

The main objective of this thesis is to explore how cells capable of self-renewal manage accumulated damaged proteins. To do this *in vivo* an immunohistochemical approach was taken, which allows for the identification of damaged proteins within stem/progenitors residing within their niche. One limitation of this approach is the difficulty of tracking damaged proteins within cells over time to discover how they influence cell function. To overcome this limitation cells capable of self-renewal and differentiation, and which can be induced to express Htt-GFP, were observed over time *in vitro* using live-imaging. Understanding how damaged proteins are inherited during a self-renewing division has important implications for the fields of aging and disease. The studies presented in this thesis will aid efforts to reduce the effects of aging by decreasing the amount of damaged proteins in stem/progenitor cells and develop novel cancer treatments.

Specific aims and hypotheses

1) Damaged proteins will be segregated to the cell with the shortest functional lifespan when a stem/progenitor cell divides asymmetrically to self-renew and produce differentiated progeny.

To determine how stem/progenitor cells manage damaged proteins during mitosis *in vivo*, I will describe the localization of damaged proteins in GSC, ISC, and NB in Chapter 2. Similar to yeast and bacteria, I expect that damaged proteins will be

asymmetrically segregated during mitosis. Furthermore, I predict that the functional lifespan of the progeny, and not self-renewal capability, will determine the cell that receives the majority of damaged proteins during cell division.

2) Damaged protein inheritance depends on both cell-extrinsic and -intrinsic mechanisms.

Using the same three stem cell populations, I will test how damaged proteins are segregated to one cell during mitosis (Chapter 2). The importance of the niche on damaged protein localization will be tested by mechanical disruption and in mutants that contain self-renewing cells removed from the stem cell niche. I propose that both the niche and cell-intrinsic factors have a role in polarization of damaged proteins within stem/progenitor cells.

3) The aggregation status and inheritance of damaged proteins affects cell fate.

The functional significance of damaged proteins existing as diffuse molecules or in aggregates will be investigated *in vitro* with respect to proliferation, cell death, and resistance to oxidative stress (Chapter 3). Furthermore, live-imaging will be used to determine if there is a difference in cell fate between the progeny of an asymmetrically dividing cell containing a damaged protein aggregate.

CHAPTER 2

The asymmetric segregation of damaged proteins is stem cell-type dependent

A version of this chapter has been published:

Bufalino, M.R., B. DeVeale, D. van der Kooy. 2013. The asymmetric segregation of damaged proteins is stem cell-type dependent. *J. Cell Biol.* 201:523-30

Summary

Asymmetric segregation of damaged proteins during mitosis has been linked in yeast and bacteria to the protection of one cell from aging. Recent evidence suggests that stem cells may employ a similar mechanism; however, to date there is no *in vivo* evidence demonstrating this effect in healthy adult stem cells. We report that stem cells in larval (neuroblast) and adult (female germline and intestinal stem cell) *Drosophila* asymmetrically segregate damaged proteins, such as proteins with the difficult-to-degrade and age-associated 2,4-hydroxynonenal (HNE) modification. Surprisingly, of the cells analyzed only the intestinal stem cell protects itself by segregating HNE to differentiating progeny, whereas the neuroblast and germline stem cells retain HNE during division. This led us to suggest that chronological lifespan, and not cell type, determines the amount of damaged proteins a cell receives during division. Furthermore, we reveal a role for both niche-dependent and -independent mechanisms of asymmetric damaged protein division.

Introduction

Aging at the cellular level is generally characterized by a decline in cell function and has been correlated with the accumulation of cellular components, such as proteins, damaged by ROS (Giorgio et al., 2007). Despite the recent focus on the impact of aging stem cells on organism health, no studies have addressed whether adult stem cells are capable of resetting their age by directing damaged proteins to differentiating progeny.

So far, the most well studied systems of the asymmetric segregation of damage, which include ROS-damaged DNA, proteins, and lipids, are bacteria and yeast (Lindner et al., 2008; Aguilaniu et al., 2003; Shcheprova et al., 2008). Protein aggregates in *E. coli* accumulate in the old-pole of the cell with age and are associated with a decreased growth rate (Lindner et al., 2008). In yeast, carbonylated proteins and extrachromosomal ribosomal DNA circles (ERC's) are retained by the mother cell during asymmetric division, while the daughter bud cell is rejuvenated (Aguilaniu et al., 2003; Shcheprova et al., 2008). This unequal partitioning of damaged proteins during mitosis appears to be a well-conserved phenomenon, also found for proteins destined for degradation in human embryonic and mammalian fibroblast cell lines (Fuentealba et al., 2008). Furthermore, huntingtin is polarized during division when it is expressed in human embryonic and mammalian somatic cell lines and embryonic *Drosophila* neuroblasts (Rujano et al., 2006).

To determine if the asymmetrical segregation of damaged proteins is conserved in a non-diseased state *in vivo*, we probed for proteins directly modified on a histidine residue by an endogenous marker of damaged proteins, HNE. HNE is a product of lipid

peroxidation that is highly reactive and readily forms covalent bonds with proteins that have been oxidized, making them resistant to proteolysis through the proteasome, although they are susceptible to lysosomal degradation (Friguet and Szweda, 1997; Marques et al., 2004). HNE has previously been identified as an indicator of oxidative stress, contains carbonyl groups (a post-translational modification that can effect the catalytic activity of proteins and increases with age), and identifies a wider range of proteins than another indicator of lipid peroxidation, malondialdehyde, and a method to identify carbonylated proteins using dinitrophenyl hydrazone (Toroser et al., 2007). Furthermore, increased levels of lipid peroxidation products are common to many neurodegenerative diseases (Butterfield et al., 2011).

Using HNE as an indicator of damaged proteins, we assessed its asymmetric segregation in the female germline stem cell (GSC), adult intestinal stem cell (ISC) and larval neuroblast (NB) of *Drosophila*. Each ovary is made up of approximately 20 ovarioles, each containing one germarium. Two to three GSCs are anchored to cap cells, which maintain the stem cells by secreting bone morphogenetic protein (BMP) that suppresses transcription of a differentiation gene, *bag-of-marbles* (Fuller and Spradling, 2007). Through asymmetric division, GSCs self-renew and create a cystoblast (CB) that goes through four rounds of division with incomplete cytokinesis to finally generate a 16-cell cyst (Kirilly and Xie, 2007) (Fig. 1D, example Fig. 1C). ISCs replace the differentiated cells of the posterior midgut approximately every week. ISCs self-renew and produce an enteroblast (EB), which differentiates into either an enterocyte or enteroendocrine cell (Micchelli and Perrimon, 2006; Ohlstein and Spradling, 2006) (Fig. 1F, example Fig. 1E). NBs divide asymmetrically to self-renew and produce a ganglion

mother cell (GMC), which then generally divides symmetrically to create the neurons of the adult brain (Fig. 1H, example Fig. 1G).

Materials and methods

Flies

Wildtype Oregon R flies were raised on standard cornmeal/sugar/yeast/agar diet at 25°C with 50% relative humidity on a 12-hour light-dark cycle. *bam*^{Δ86} (Bloomington Stock Center, Indiana University) and *raps*¹⁹³ (Bloomington Stock Center, Indiana University) flies were maintained in the same conditions as wildtype. *N^{TS1}* flies (Bloomington Stock Center, Indiana University) were maintained at 21°C and moved to 29°C for 10 d during experiments. *Gbe⁺Su(H)LacZ* flies (a kind gift of Dr. Benjamin Ohlstein; Furriols and Bray, 2001) were maintained in the same conditions as wildtype. For the comparison of ISCs and adjacent EBs during aging, flies were transferred to medium (5% sucrose, 5% yeast extract, 0.5% agarose) that contained 0.2 mg/mL BrdU, 4 d prior to the aging time point (Invitrogen sheep anti-BrdU was used at 1:50). Paraquat (methyl viologen dichloride hydrate) was obtained from Sigma and dissolved in a 5% sucrose solution to make a 10 mM paraquat solution. Wildtype flies 10d after eclosion were fed paraquat for 24h at 25°C in the dark.

Immunohistochemistry

All tissues were dissected in Schneider's *Drosophila* medium, rinsed with PBS and then fixed for 20 min in Bouin's fixative and washed for 20 min in 70% ethanol. Ovaries and larval brains were sectioned at 6 and 10 μm , respectively, prior to staining. Blocking was performed for 1 h at RT in 5% normal goat serum solution of PBS with 0.2% Triton X-100. Tissue was incubated in primary antibodies at 4°C overnight in PBS/ 1% normal goat serum/ 0.2% Triton X-100 and after three washes (PBS/ 0.2% Triton X-100) in secondary antibodies for 2 h at RT in PBS/ 1% normal goat serum/ 0.2% Triton X-100. Alternatively, ovaries in the aging experiment were stained as whole-mounts after 10 min incubation in a 0.05% trypsin solution with 1% calcium chloride at 37°C, with incubation in primary and secondary antibodies increased to two nights on a shaker. To stain membranes, 2.5 $\mu\text{g}/\text{mL}$ Fast DiI (Invitrogen) was applied to tissues for 1 h at 4°C following trypsin treatment and tissues were permeabilized with 0.3% Tween-20 in phosphate buffered saline for 2 h at 4°C prior to immunohistochemistry. To stain intestines, the entire gastrointestinal tract was dissected and then stained as previously described for larval brain and ovary tissue with the exceptions that tissue was not sectioned, blocking was increased to 3 h at 4°C, and primary antibodies were washed for 2 h at 4°C prior to incubation with secondary antibodies for 3 h at 4°C. The following primary antibodies were used with appropriate alexa-conjugated secondaries (1:300) followed by Hoescht 33258 (1:1000, Sigma) for 10 min at RT: mouse anti-HNE (20 $\mu\text{g}/\text{mL}$; R&D Systems, discontinued), rabbit anti-HNE (1:50; abcam), rabbit anti-Histone H3 (1:100, abcam), mouse anti-polyubiquitin (1:100; BIOMOL International), mouse

anti-mono- and poly-ubiquitinated proteins (1:100; BIOMOL International), rat anti-Elav (1:10, Developmental Studies Hybridoma Bank (DSHB)), rabbit anti-PKC ζ (1:1000, C20, Santa Cruz Biotechnology Inc), mouse anti- α -spectrin (1:20, DSHB), chicken anti- β -galactosidase (1:1000, abcam), mouse anti-delta (1:10, DSHB), mouse anti-Prospero (1:10, DSHB), rat anti-DE-Cad (gut and ovary, 1:20, DSHB), rat anti-DE-Cad (larval brain, 1:500, a kind gift of Volker Hartenstein), and rat anti-Vasa (1:4, DSHB). All samples were mounted in an aqueous mounting medium (Fluoro-Gel, Electron Microscopy Sciences). Images were captured at room temperature with the Olympus DP72 12.8 megapixel cooled digital color camera using a 60x (numerical aperture: 0.85) water immersion objective of a confocal laser scanning microscope (FV1000, Olympus). The following fluorochromes were used: Alexa 405, 488, 568 and 647. Brightness and contrast of entire images were adjusted with FV1000 software.

Neuroblast cell culture

Brains were removed from L3 larvae and immediately placed in Schneider's medium supplemented with 5% fetal bovine serum. The ventral nerve cord was removed and the central brain and optic lobe were mechanically dissociated, using the tips of 30 1/2 gauge needles, in poly-d-lysine coated cover slip bottom dishes (MatTek Corp.). After allowing cells to adhere to the dish for 20 min at 25°C in the dark they were rinsed with PBS prior to fixing for 20 min and staining exactly as larval brain slices with the exception that cells were counterstained with 2 X Hoescht 33258.

Image analysis

ImageJ was used to analyze all images. ISCs were identified as small cells in mitosis unless otherwise noted. *raps¹⁹³/raps¹⁹³* mutant NBs were identified as nuclear Prospero-negative cells that were no more than 15% larger than adjacent Prospero-positive cells. All staining intensity measurements are presented as pixel intensity subtracted by average background. Average cytoplasmic staining, used to compare stem cells and adjacent progeny, was measured by drawing boundaries around the nucleus as identified by Hoescht staining (Fig. 6). Average background was calculated by averaging areas of minimal pixel intensity within the tissue being analyzed or the cell culture plate. The distribution of staining within a cell was calculated by generating a plot profile for each cell and then averaging the pixel intensity contained in opposite ends of the cell. Each end was separated by the nucleus, which contained minimal staining and was standardized as the center 30% of the GSC and ISC and 60% of the NB.

Statistical analysis

Paired two-tailed Student's *t*-tests were used to analyze localization measurements and compare adjacent cells and a one-way ANOVA was used to determine the effect of age on staining. A Chi-square test was used to determine if the frequency of NBs with different amounts of HNE asymmetry varied between cells in prophase and metaphase/anaphase. Results were considered statistically significant when $P < 0.05$. All statistical tests were completed using Prism 4 (GraphPad Software Inc.). A cell was

classified as asymmetric if HNE content was $\geq 35\%$ greater on the side of the cell predicted to have greater staining or UP content was $\geq 20\%$ greater.

Results and discussion

HNE is a marker of damaged proteins that accumulate with oxidative stress and age

To validate HNE as a marker for damaged proteins, GSCs were assessed after exposure to oxidative stress and aging. Flies (10 d after eclosion) were treated for 24 h with either a xenobiotic that induces ROS production upon ingestion (10 mM paraquat) in 5% sucrose or 5% sucrose alone at 25°C. GSCs have greater (3.0-fold) HNE staining in paraquat-treated compared to sucrose treated flies ($p < 0.05$; Fig. 5E, examples Fig. 5F,G). HNE has been found to accumulate with age in *Drosophila* flight muscles (Toroser et al., 2007) and through the modification of proteins contributes to general cell dysfunction associated with aging (eg. HNE disrupts DNA synthesis, protein production, enzyme function and the ability of cells to communicate through gap junctions) (Okada et al., 1999). Ovaries stained for HNE and α -tubulin as a control revealed that average HNE intensity increases significantly with age in GSCs (Fig. 1A, examples Fig. 5C; $p < 0.05$ by one-way ANOVA), with a 2.75-fold increase between 5 and 45 d. Therefore, HNE represents a protein modification associated with oxidative stress and age. Unexpectedly, ISCs did not display a significant increase in HNE with age when identified as small cells in mitosis (Fig. 1B, examples Fig. 5D; $n \geq 10$ for each time point, $p > 0.05$ by one-way ANOVA) and as the smallest cell in a BrdU+ lineage (Fig. 5B; $n \geq 8$ for each time point,

$P > 0.05$ by one-way ANOVA). This unexpected difference in the extent of HNE accumulation with age between GSCs and ISCs, prompted us to look at other differences in stem cell populations with respect to HNE.

Figure 1

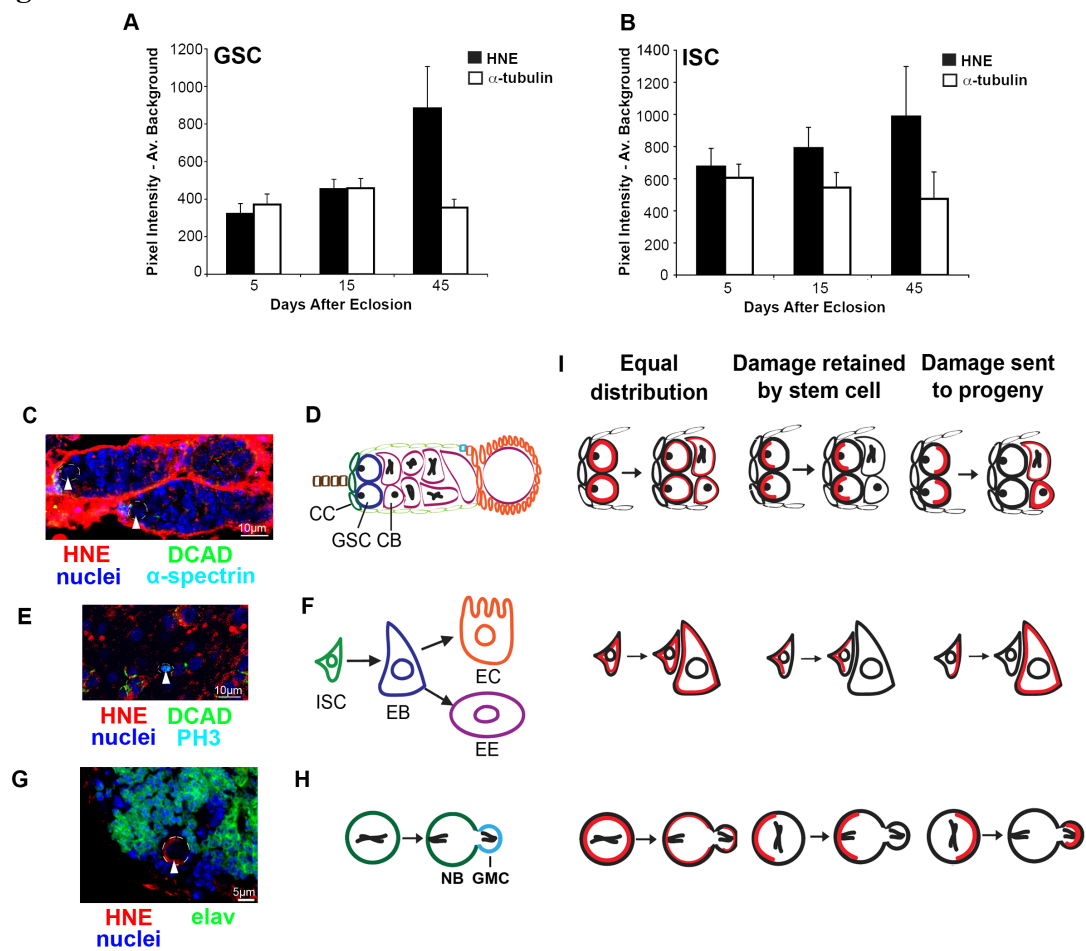


Figure 1. GSCs accumulate more HNE with age compared to ISCs, indicating separate modes of HNE distribution during mitosis

(A) GSCs accumulate HNE during aging ($n = 10$ for each time point). (B) Contrary to the GSC, HNE does not accumulate significantly with age in ISCs ($n \geq 10$ for each time point). (C+D) Each germarium contains GSCs (arrowheads), which reside adjacent to cap cells (CC) and divide asymmetrically to give rise to CBs. (E+F) ISCs (arrowhead) self-renew and produce an EB, which can differentiate into an enterocyte (EC) or enteroendocrine cell (EE). (G+H) NBs (arrowhead) divide asymmetrically to self-renew and produce a GMC, which generally divides to give rise to neurons. (I) Potential types of damaged protein (red) segregation are shown in the GSC (upper panel), ISC (center panel), and NB (lower panel). For all figures, the mean (\pm s.e.m.) represents HNE (or alternative stain) pixel intensity subtracted by average background and asterisks indicate $p < 0.05$ by paired two-tailed t -test.

Stem cells and progeny differ in HNE levels

HNE-modified proteins in GSCs, NBs, and ISCs may be uniformly distributed within stem cells, or polarized to one end of the cell, leading to their asymmetric segregation during mitosis (Fig. 1I). Based on the accumulation of HNE in GSCs with age, it was predicted that GSCs, but not ISCs retain damaged proteins at division. As a result of polarized HNE, stem cells and adjacent progeny should differ in HNE levels. GSCs exceed adjacent progeny (2.8-fold) in average cytoplasmic HNE intensity ($p < 0.05$, paired two-tailed t -tests; Fig. 2D; example Fig. 2A). This trend is conserved during aging; GSCs have significantly more HNE than CBs at each time point ($p < 0.05$, paired two-tailed t -tests; Fig. 5A) and HNE content in CBs does not significantly increase with age ($P > 0.05$, one-way ANOVA; Fig. 5A; examples Fig. 5C). Similar to GSCs, NBs have greater (4.27-fold) average cytoplasmic HNE intensity than adjacent neurons ($p < 0.05$; Fig. 2F; example Fig. 2B). In contrast, there is significantly reduced (3.73-fold) average HNE staining in ISCs compared to adjacent progeny ($p < 0.05$; Fig. 2H; example Fig. 2C). This trend is conserved during aging; ISCs (identified as the smallest BrdU-positive cell in a BrdU-positive cell cluster) have significantly less HNE than adjacent EBs at each time point ($p \leq 0.05$, paired two-tailed t -tests; Fig. 5B). To confirm that EBs contain more HNE than ISCs, EBs were identified as β -galactosidase-positive cells in $Gbe^+Su(H)lacZ$ flies (Furriols and Bray, 2001), and found to contain 1.54-fold greater HNE than adjacent small β -galactosidase-negative cells ($p < 0.05$; Fig. 5S; example Fig. 5R).

Intracellular HNE distributes asymmetrically

In support of asymmetric segregation, each stem cell type contains polarized HNE staining. GSCs contain significantly more HNE in the region adjacent to cap cells during interphase (2.47-fold, $p < 0.05$; Fig. 2E) and mitosis (2.1-fold, $p < 0.05$; Fig. 2I). This result was confirmed using a second HNE antibody, which has 1.97-fold greater HNE on the cap cell side of the GSC during interphase ($p < 0.05$; Fig. 5H; example Fig. 5I). Similar to GSCs, NBs contain greater HNE staining in the area farthest from adjacent progeny during interphase (3.32-fold, $p < 0.05$; Fig. 2G) and mitosis (19.2-fold, $p < 0.05$; Fig. 2J). Regions of high DE-Cadherin (DCAD) staining were used to predict the side of an ISC that would form the EB; the point of contact between ISCs and EBs is rich in β -catenin and DCAD (Maeda et al., 2008). In ISCs greater HNE staining (6.49-fold) is found in regions of high DCAD expression during mitosis ($p < 0.05$; Fig. 2K). Therefore, HNE is localized to the side of the ISC most likely to contribute to the EB.

Ubiquitinated proteins (UPs) are marked for degradation through the proteasome and similar to HNE, are detected in neurodegenerative diseases (Vernace et al., 2007). The same trend of intracellular accumulation identified for HNE was found for UPs in the GSC (1.58-fold, $p < 0.05$, Fig. 5J, example 5M), NB (1.24-fold, $p < 0.05$, Fig. 5K, example 5N) and ISC (1.5-fold, $p < 0.05$, Fig. 5L, example 5O). UPs also co-localize with a NB polarity protein, PKC ζ , to the side opposite of GMC production with 1.87-fold greater UP staining during mitosis ($p < 0.05$; Fig. 5P; example Fig. 5Q). This suggests that asymmetric segregation exists for damaged proteins with different modifications.

Based on the intracellular localization data we suggest that chronological lifespan, and not cell type, determines the amount of damaged proteins a cell receives during division. The GSC is shorter-lived than its CB progeny because the CB can form a new organism with the ability to outlive the mother where the GSC resides. Similarly, the NB undergoes apoptosis or differentiates into unknown cell types during pupation making it shorter-lived than its neuronal progeny, which persist to adulthood (Chell and Brand, 2008). Therefore GSCs and NBs protect their longer-lived differentiating progeny by retaining a factor associated with aging. This is distinct from ISCs, present throughout the organisms' lifespan, that segregate HNE towards differentiating progeny, which are replaced approximately every week (Micchelli and Perrimon, 2006; Ohlstein and Spradling, 2006).

Figure 2

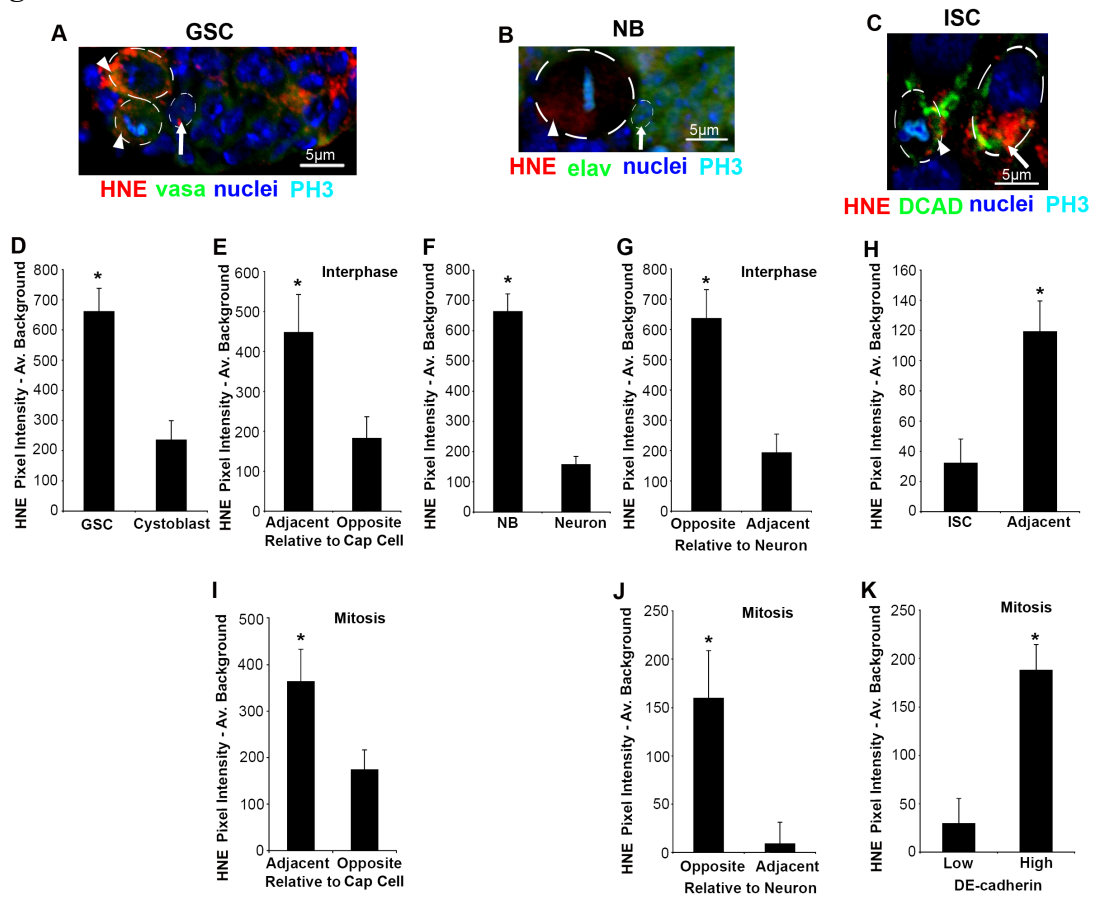


Figure 2. HNE is asymmetrically distributed in the GSC, NB, and ISC

(A) Example of a germarium containing GSCs (arrowhead) and adjacent CB (arrow). (B) Example of a NB (arrowhead) with polarized HNE that contains greater HNE content than adjacent neurons (arrow). (C) Example of an ISC (arrowhead) with an asymmetric distribution of HNE and adjacent differentiated cell (arrow). (D) GSCs contain significantly more damage (HNE) than adjacent cells (CBs or cystocytes) ($n = 11$) and during interphase HNE is localized to the site opposite of CB production ($n = 11$; E; 11/11 cells asymmetric). (F) Similar to the GSC, the NB contains more HNE than adjacent progeny ($n = 16$) and during interphase HNE is localized to the site opposite of new neurons ($n = 10$; G; 9/10 cells asymmetric). (H) In contrast, ISCs contain less damage than adjacent differentiated cells ($n = 10$). During mitosis HNE asymmetry is maintained in the GSC ($n = 8$; I; 6/8 cells asymmetric) and NB ($n = 12$; J; 11/12 cells asymmetric). (K) ISCs also have polarized HNE during mitosis, when the cell is separated based on DCAD staining intensity ($n = 10$; 10/10 cells asymmetric).

In each stem cell population HNE associates with a niche adhesion molecule

DCAD has important roles in the niche of all three stem cell systems (Song et al., 2002; Dumstrei et al., 2003; Maeda et al., 2008) and is involved in the asymmetric division of *Drosophila* male GSCs through its effects on spindle orientation (Inaba et al., 2010). GSCs in interphase contain greater DCAD (122.8-fold) and HNE (17.7-fold) adjacent to cap cells ($p < 0.05$ for both; Fig. 3C; example Fig. 3A). Within NBs in interphase, more DCAD (9.5-fold) and HNE (3.38-fold) are found opposite neuron production ($p < 0.05$ for both; Fig. 3D; example Fig. 3B). Therefore, despite the differences in damaged protein distribution with respect to differentiating progeny, HNE and DCAD co-localize in all three stem cell populations.

Figure 3

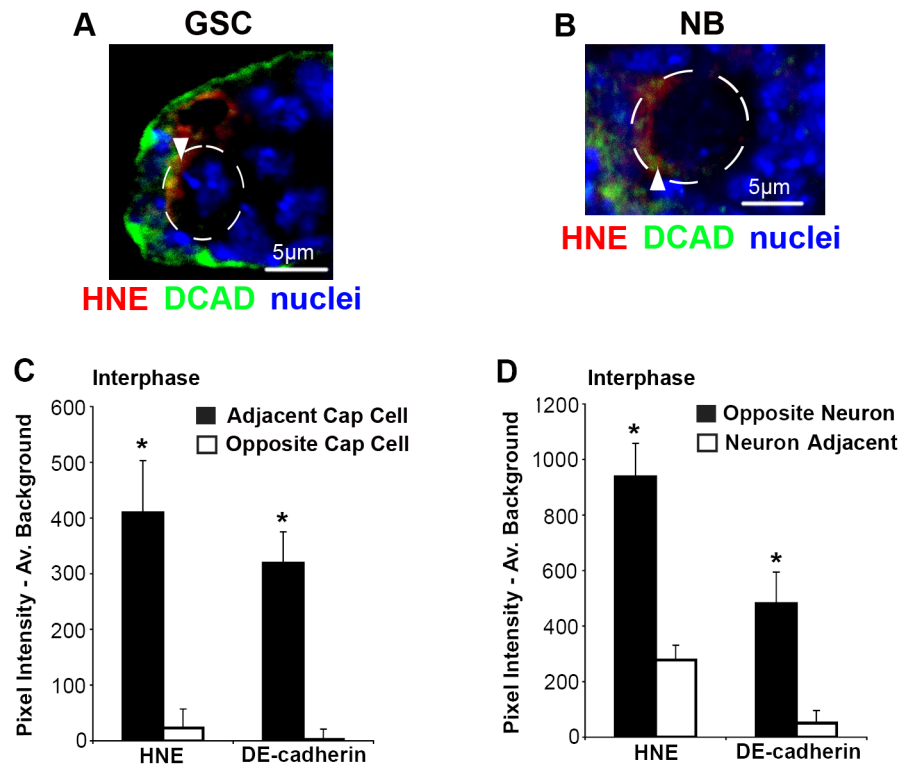


Figure 3. DCAD and HNE co-localize

Examples of regions of intense DCAD staining that colocalize with areas of high HNE staining (arrowhead) in the GSC (A) and NB (B). Similar to ISCs (Fig. 2K), within GSCs ($n = 11$; C; 10/11 cells asymmetric) and NBs ($n = 9$; D; 9/9 cells asymmetric) there is significantly more HNE and DCAD at the side of the cell opposite to new differentiating progeny during interphase.

GSCs displaced from their niche lose some but not all HNE polarization

The progeny of GSCs require the expression of a differentiation-promoting gene, *bam*, to differentiate, and in its absence the germarium is filled with undifferentiated GSC-like cells. A deletion mutant, *bam*^{Δ86} (McKearin and Ohlstein, 1995), was used to determine the effect of contact with stem cell niche cells on the localization of HNE within stem cells. *bam*^{Δ86}/*bam*^{Δ86} flies maintained at 25°C for 20 d, displayed an accumulation of undifferentiated cells with a spectrosome, an organelle rich in membrane skeleton proteins that anchors the mitotic spindle (Deng and Lin, 1997), indicated by α -spectrin staining (Fig. 4A; channels separated in Fig. 7A). Undifferentiated cells in interphase within the GSC niche with high DCAD content contain 1.71-fold greater HNE adjacent to cap cells ($p < 0.05$; Fig. 4B; example Fig. 4A and 7A). Undifferentiated cells at least two cells away from the GSC niche, also displayed polarized HNE during interphase; however, not to the same extent as those cells within the niche. These cells contained 1.42-fold greater HNE at the side of the cell with the spectrosome ($p < 0.05$; Fig. 4C; example Fig. 4A and 7A).

The spectrosome is associated with the centrosome (Lin et al., 1994); therefore, the centrosome may be involved in damaged protein polarization. Accumulated misfolded proteins actively localize to the aggresome, a structure associated with the spindle-pole body in yeast (Wang et al., 2009) and centrosome in *Drosophila* and mammals (Rujano et al., 2006). Still, the extent of HNE polarization was greatest in cells within the niche, suggesting that baseline levels of HNE do not depend exclusively on centrosome association for their asymmetric distribution.

The extent of DCAD polarization predicts HNE asymmetry in ISCs

The fate of ISC progeny depends on Notch signaling, with high levels of Delta leading to EC and low levels to enteroendocrine cell production (Ohlstein and Spradling, 2007). To assess the effect of niche disruption on the asymmetrical distribution of damaged proteins in ISCs, we employed a temperature-sensitive Notch mutant (N^{TS1} ; Shellenbarger and Mohler, 1975), which produces clusters of delta-positive ISC-like cells when cultured at 29°C for 10 d (Fig. 4D; channels are separated in Fig. 7B). HNE remains localized to DCAD within ISC-like cells in interphase. Cells within clusters were separated into low and high DCAD polarization (2x greater polarity than low condition). In low DCAD polarity cells, no significant polarization of HNE is found ($p > 0.05$; Fig. 4E), and in high DCAD polarity cells HNE remains localized (2.28-fold) to regions of intense DCAD during interphase ($p < 0.05$; Fig. 4E; example Fig. 4D). Therefore, when an ISC-like cell is in an environment similar to the stem cell niche (high DCAD polarization) damaged protein localization is preserved.

Both niche-dependent and -independent factors are responsible for HNE polarization in NBs

NBs can be mechanically dissociated from their niche and within 20 min of being in cell culture and with no cell-cell contact, except for a small cluster of cells containing neurons, show no significant asymmetric localization of HNE to the side of the NB opposite neurons ($p > 0.05$; Fig. 4J; examples Fig. 4F,G). Surprisingly, HNE becomes

increasingly localized to one region of mitotic NBs as the cell cycle progresses; more NBs in metaphase and anaphase contain a greater difference in HNE staining between two sides of the cell than those in prophase ($p < 0.05$ by Chi-Square Test; Fig. 4K; examples Fig. 4H,I). This finding supports the existence of a niche-independent mechanism of damaged protein segregation, such as the polarisome. In yeast, the polarisome is responsible for retrograde transport of protein aggregates along actin cables from the bud to the mother during cell division (Liu et al., 2010) and a similar mechanism may be conserved in *Drosophila*. Interestingly, the extent of HNE polarization in mitotic NBs in culture does not reach that of cultured NBs in interphase (13% vs. 28%), if the cell is divided based on pixel intensity instead of neuron position (Fig. 4K). This finding suggests that the plane of polarization may be reset during mitosis and that the niche is needed to reach the maximum level of polarization.

Alternatively, damaged proteins may accumulate in NBs because they are larger than daughter GMCs or because they are associated with the mitotic spindle, like many polarity proteins in the NB. We explored these possibilities using a mutant of Rapsynoid/Partner of Inscuteable (Raps), a cortical polarity protein in the NB responsible for spindle orientation and size of daughter cells (Siller et al., 2006). In the *raps¹⁹³/raps¹⁹³* mutant the large size difference between NBs and GMCs and the asymmetric distribution of proteins normally localized to the NB (Inscuteable) and GMC (Miranda) are disrupted (Parmentier et al., 2000); however, NBs can be distinguished from GMCs by their absence of nuclear Prospero. We found that *raps¹⁹³/raps¹⁹³* mutant NBs in interphase contain significantly greater HNE content, 1.50-fold, than adjacent progeny ($p < 0.05$; Fig. 4M; example Fig. 4L). On average, the Prospero-negative cells were only

1.9% larger than adjacent Prospero-positive cells; therefore, damaged proteins do not accumulate in NBs due to their large size or association with the mitotic spindle and future studies should examine other mechanisms of asymmetric distribution, such as the polarisome.

Conclusions

Damaged proteins are polarized in GSCs, NBs, and ISCs and inherited by the cell with the shortest functional lifespan (GSC, NB and EB), which may defend against one cause of aging, the build-up of molecules damaged by ROS (Giorgio et al., 2007). Due to the deleterious effects caused by a build-up of damaged proteins, multiple mechanisms may exist to ensure their proper segregation. We found that the stem cell niche plays a role in this asymmetry, but is not the only mechanism of damaged protein segregation. We suggest that both the stem cell niche and niche-independent mechanisms are responsible for the asymmetric segregation of damaged proteins.

Figure 4

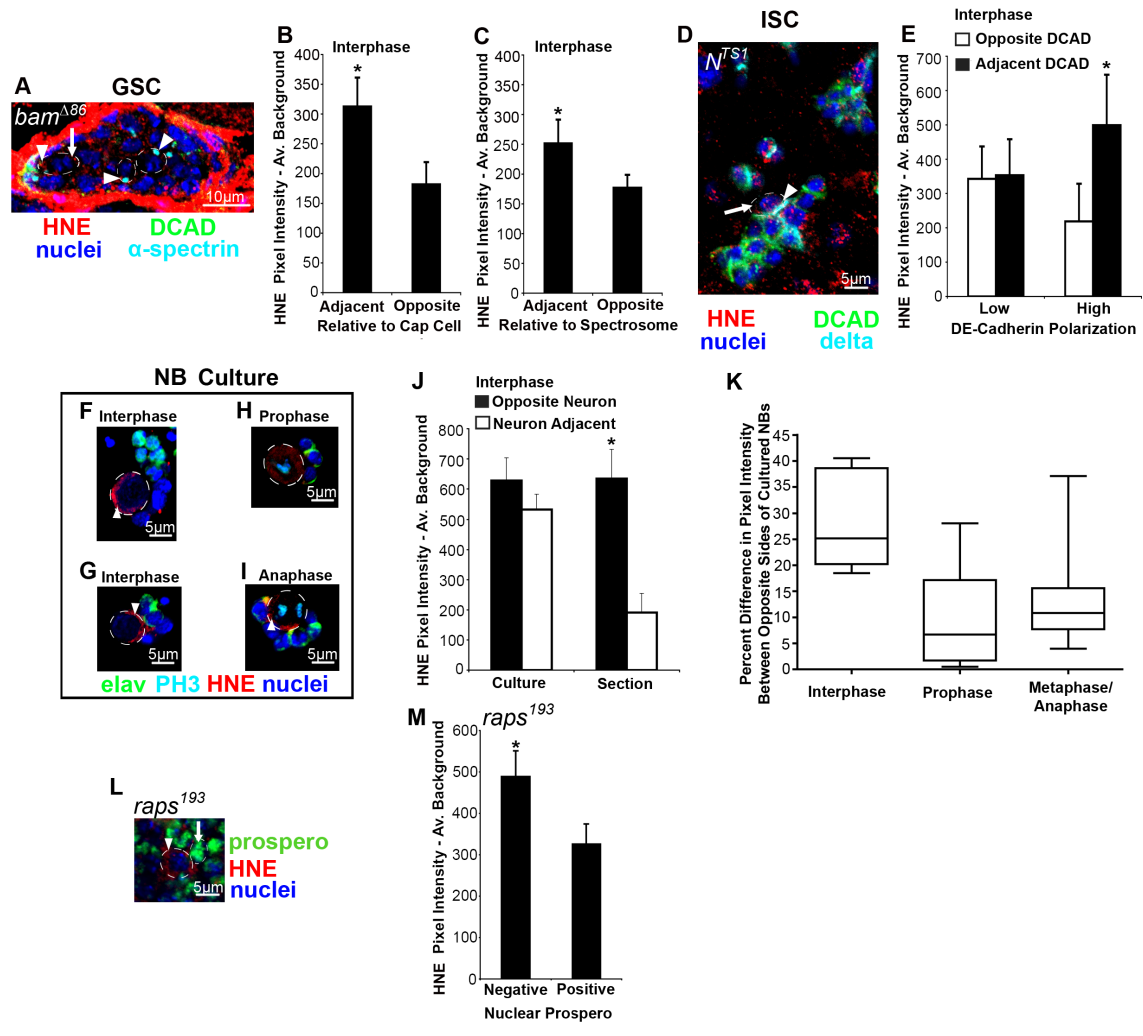


Figure 4. The niche is involved in HNE asymmetry

(A) Example of a $bam^{\Delta 86}/bam^{\Delta 86}$ germarium where GSC-like cells contain polarized HNE in both cells adjacent to the stem cell niche (arrowhead indicates region adjacent to cap cells and arrow indicates opposite region) and at least two cells removed from the niche (arrowheads). (B) HNE remains localized to the anterior end of cells in interphase within the GSC niche in $bam^{\Delta 86}/bam^{\Delta 86}$ germariums ($n = 12$; 12/12 cells asymmetric). (C) Cells in $bam^{\Delta 86}/bam^{\Delta 86}$ germariums, which have intense HNE staining and are at least two cells away from the niche, also display polarized HNE during interphase that localizes to the spectrosome ($n = 10$; 6/10 cells asymmetric). (D) Examples of delta-positive clusters of ISC-like cells within a N^{TS1}/N^{TS1} midgut. Arrowhead indicates region of intense DCAD staining that co-localizes with the most intense region of HNE staining compared to opposite side (arrow). (E) Only cells within delta-positive N^{TS1}/N^{TS1} cell clusters with a high level of DCAD polarization contain an asymmetric distribution of HNE during interphase ($n = 9$; 9/9 cells asymmetric). Cells with low (2x less) DCAD polarization do not have an asymmetric distribution of HNE during interphase ($n = 7$; 1/7 cells asymmetric). (F+G) Examples of cultured NBs (circled) in interphase; HNE does not consistently localize to the side of the cell opposite neurons. (J) Asymmetric HNE localization to the side of NBs opposite adjacent neurons is lost when the NB niche is disrupted during cell culture ($n = 8$; 1/8 cells asymmetric). (K) The polarization of HNE increases in mitotic cells with cell cycle progression (prophase, $n = 15$, example in H; metaphase and anaphase, $n = 17$, example in I; interphase $n = 8$). (M) Symmetrically dividing NBs in $raps^{193}/raps^{193}$ mutants (arrowhead) identified as Prospero-negative cells

contain greater HNE staining than adjacent cells (arrow) of a similar size during interphase ($n = 9$, example in L).

Figure 5

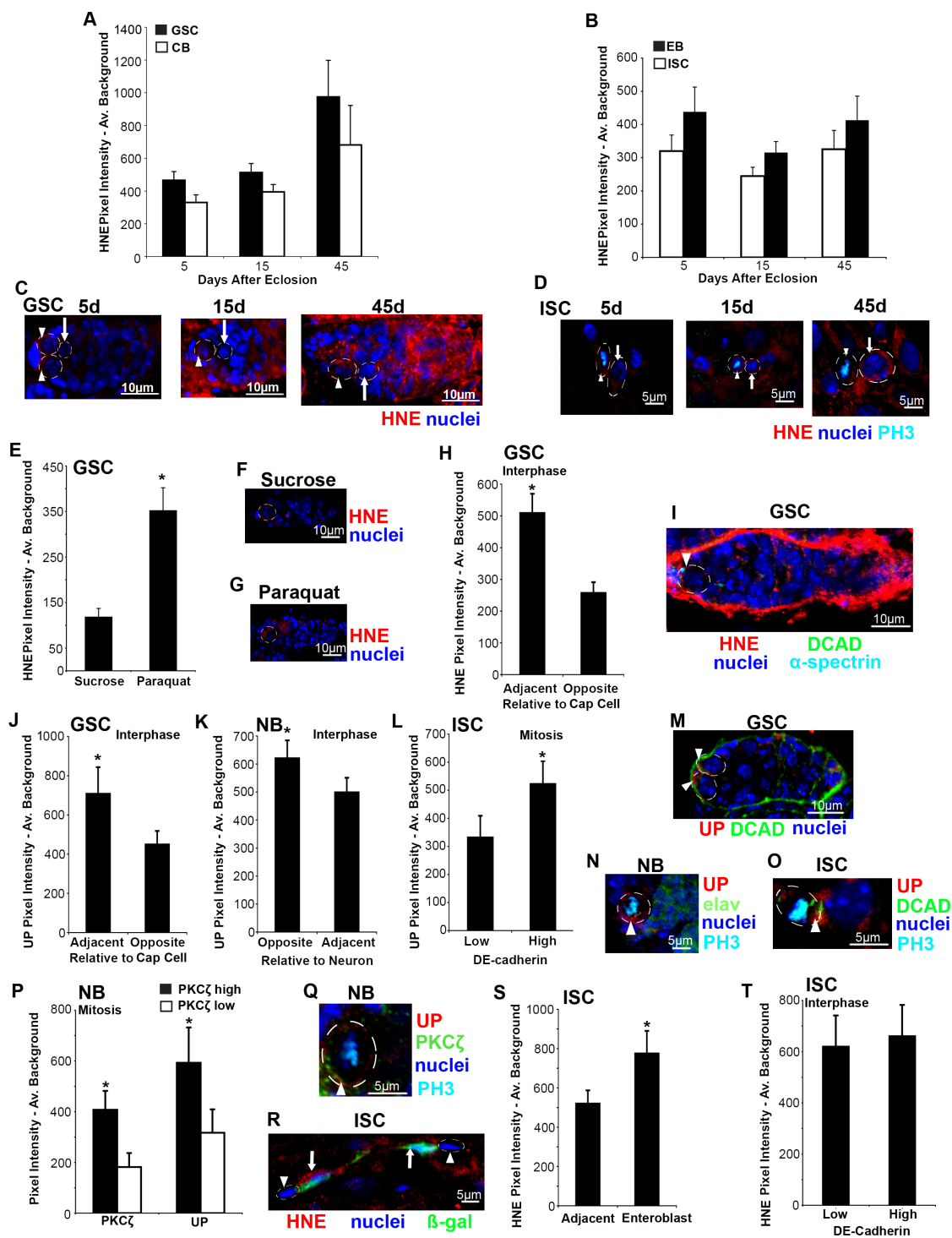


Figure 5. Damaged proteins in the GSC, ISC and NB

(A) GSCs contain greater HNE content than adjacent CBs during aging ($n \geq 8$ for each time point). (B) ISCs, identified as the smallest cell in a BrdU positive lineage, contain less HNE content than adjacent EBs during aging ($n \geq 8$ for each time point). (C) Examples of GSCs (arrowhead) and CBs (arrow) during aging. (D) Examples of ISCs (arrowhead) and EBs (arrow) during aging. (E) Significantly greater HNE content is found in GSCs of flies fed on paraquat for 24 h compared to the sucrose control ($n = 8$). Examples of GSCs (circled) in the sucrose (F) and paraquat (G) conditions. (H) HNE is consistently localized to the cap cell adjacent side of GSCs in interphase using anti-HNE (abcam) ($n = 11$; 8/11 cells asymmetric, example I). Similar to HNE, ubiquitinated proteins (UPs) are asymmetrically distributed during interphase within GSCs ($n = 12$; J; 8/12 cells asymmetric), NBs ($n = 11$; K; 7/11 cells asymmetric), and during mitosis in ISCs ($n = 11$; L; 8/11 cells asymmetric). (M) Example of GSCs (arrowheads) with intense staining for UPs in the anterior tip. (N) Example of a NB (arrowhead) stained for UPs, which are found in small quantities in the L3 larval brain. (O) Example of an ISC (arrowhead) stained for UPs with adjacent progeny to the right. (P) In mitotic NBs, apical PKC ζ co-stains with asymmetrically localized UPs ($n = 8$; 7/8 cells asymmetric). (Q) Example of PKC ζ and UP co-localization in the NB, arrowhead indicates region of co-localization. (R) Example enteroblasts (arrows) and small adjacent cells (arrowheads). (S) Enteroblasts identified as LacZ positive cells from Gbe⁺Su(H)LacZ flies, contain greater levels of HNE (abcam) than small adjacent cells ($n = 15$). (T) Prior to mitosis, ISCs identified by delta staining do not display HNE accumulation on the side of the ISC

with high DCAD staining ($n = 10$; 3/10 cells asymmetric). Asterisk indicates $p < 0.05$ by paired two-tailed t -test.

Figure 6

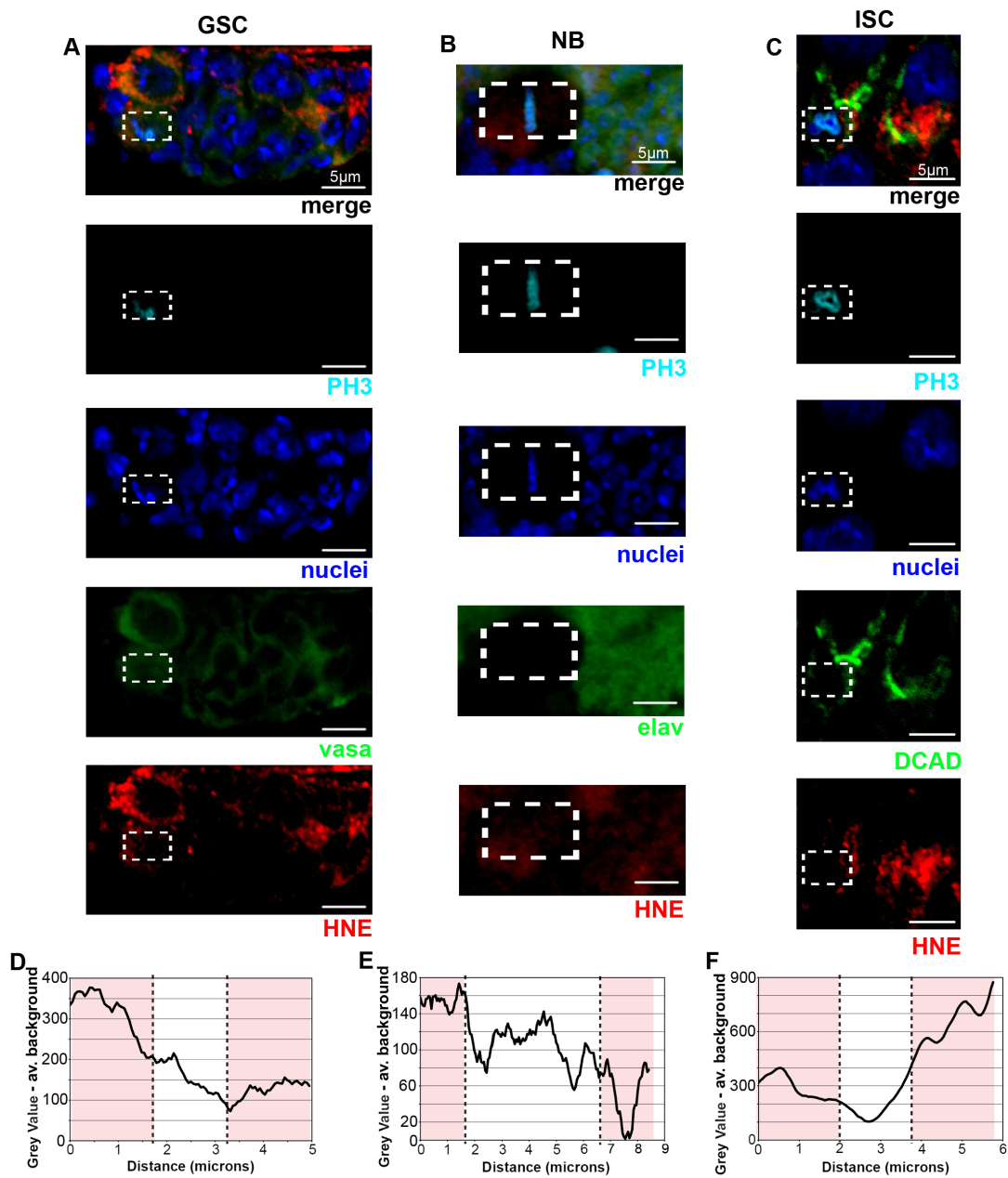


Figure 6. HNE localization measurements in the mitotic GSC, NB, and ISC.

Channels are separated for an image of a mitotic GSC (A), NB (B), and ISC (C). A plot profile is generated in ImageJ by drawing a box within the cell of interest. The program produces the profile of intensity by averaging the pixel intensity across the y-axis and plotting it against the distance (μm) on the x-axis. Across images, the nucleus is considered the center of the cell and is not included in the localization measurements. Consistent between images the center 30% of the GSC and ISC and the center 60% of NB are identified as the nuclei. The area highlighted in red of the plot profiles of HNE intensity for the GSC (D), NB (E), and ISC (F) display the regions that are included in the localization measurements. The average of each highlighted region is compared to determine the staining intensity in each region of the cell.

Figure 7

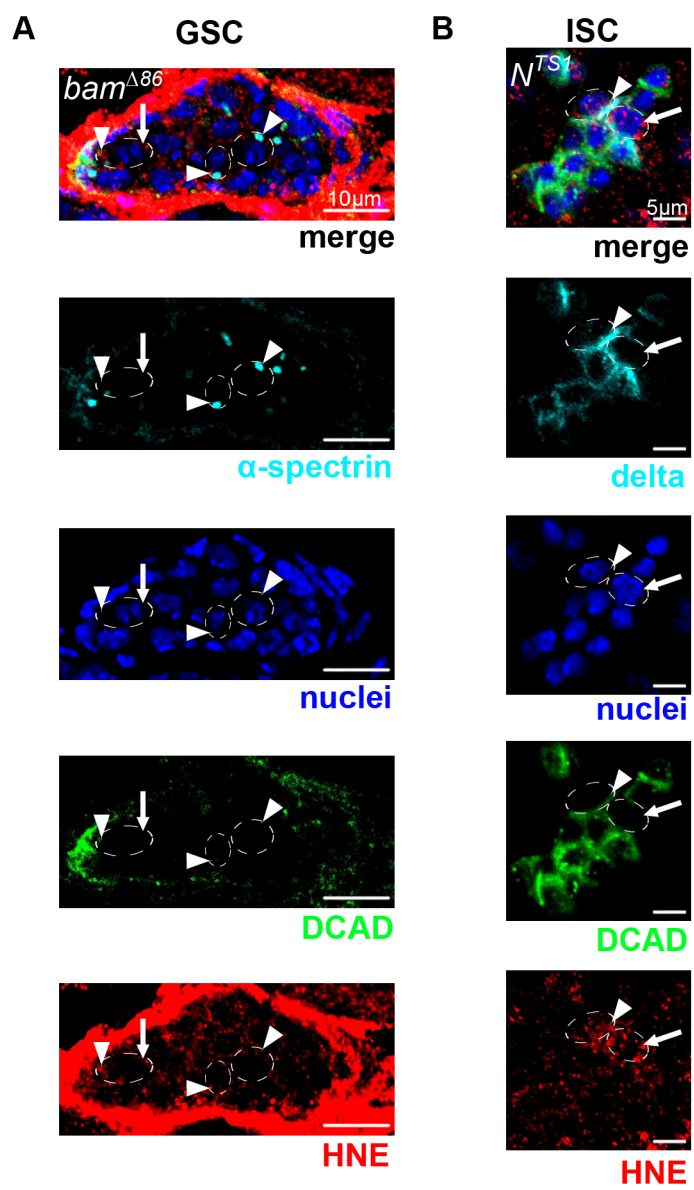


Figure 7. Localization of HNE in GSCs and ISCs removed from the stem cell niche.

(A) Channels are separated to better visualize greater levels of HNE (abcam) within the cap cell side (arrowhead) of a GSC (circled) within the niche compared to the opposite end of the cell (arrow) in a *bam*^{Δ86}/*bam*^{Δ86} germarium. In cells separated from the GSC niche, arrowheads indicate regions of cells (circled) containing a spectrosome where enriched levels of HNE (abcam) are found. (B) Channels are separated to better visualize a region of high (arrowhead) DCAD staining intensity that coincides with high HNE (abcam) staining intensity within an ISC-like cell (circled) of a *N*^{*TS1*}/*N*^{*TS1*} midgut. A cell without a strong polarization of DCAD (circled, arrow) does not contain a polarized distribution of HNE (abcam).

CHAPTER 3

The aggregation and inheritance of damaged proteins

determines cell fate during mitosis

Summary

Recent evidence suggests that proliferating cells polarize damaged proteins during mitosis to protect one cell from aging and that the structural conformation of damaged proteins mediates their toxicity. We report that the growth, resistance to stress, and differentiation characteristics of a cancer cell line (PC12) with an inducible Huntingtin (Htt) fused to enhanced green fluorescent protein (GFP) are dependent on the conformation of Htt. Cell progeny containing inclusion bodies have a longer cell-cycle and increased resistance to stress than those with diffuse Htt. Using live-imaging, we demonstrate that a symmetrically dividing cell line can be forced to divide asymmetrically when a cell contains a single inclusion body and this results in sister cells with different fates. The cell that receives the inclusion body has decreased proliferation and increased differentiation compared to its sister cell that is free of Htt. This is the first report that reveals a functional consequence of the asymmetric division of damaged proteins in mammalian cells, and we suggest that this is a result of inclusion body induced proteasome impairment.

Introduction

Aging is a complex event generally characterized by a decline in function. Recently, a review of the aging literature led to the identification of nine factors associated with aging, one of which is the loss of proteostasis (Lopez-Otin et al., 2013). In a normal cell, damaged proteins, which have been modified and no longer perform their intended function, are degraded by the proteasome, a multisubunit enzyme complex. Proteasomal activity declines with age in mice (Tomaru et al., 2012), and its role in aging appears to be well conserved as the mutations of proteasomal components result in reduced lifespan in both mice and yeast (Tomaru et al., 2012; Kruegel et al., 2011). The result of proteasomal dysfunction is the accumulation of damaged proteins that can be toxic to the cell, resulting in a decline of function. A protein can be classified as damaged when it is no longer able to perform its intended function. Both proteins improperly folded and covalently modified as a result of oxidative stress are examples of damaged proteins. As these are post-translational modifications, it is not feasible to overexpress a type of damaged protein in a cell to study its effects. Alternatively, a model of damaged proteins can be used.

Huntington's Disease (HD) is caused by an abnormal expansion (>40) of cytosine-adenine-guanine repeats in the *IT15* gene, which results in the production of abnormal Huntingtin (Htt). HD is characterized by neurodegeneration and Htt aggregates, termed inclusion bodies, both of which increase with age (Cohen et al., 2012). Similar to damaged proteins, Htt has lost its normal function, can be degraded by the proteasome, forms aggregates and indirectly impairs proteasomes and decreases a cell's ability to resist

stress (Hipp et al., 2012). For example, Htt expression in yeast with enhanced proteasomal activity results in reduced inclusion body formation compared to wildtype (Kruegel et al., 2011). Therefore, Htt provides an excellent model to study the impact of damaged proteins on cells. Initially, inclusion bodies were proposed to be responsible for the neuronal death associated with HD; however, inclusion bodies were not preferentially localized to areas of the brain that experience the greatest cell death during disease (Gutekunst et al., 1999; Kuemmerle et al., 1999) and did not predict cell death when neurons were tracked with live-imaging (Arrasate et al., 2004). This led to the theory that diffuse Htt is the more toxic conformation and inclusion bodies protect the cell from death by sequestering diffuse Htt (Arrasate et al., 2004), although this is still under debate (Todd & Lim, 2013).

So far, the toxicity of different conformations of Htt primarily has been studied in differentiated cells, as the symptoms of HD result from neuronal death. Cells capable of proliferation also are susceptible to damaged protein toxicity and it is unclear whether the conformation of damaged proteins determines their toxicity. In contrast to differentiated cells, proliferating cells can reduce damaged protein content through cell division. For example, the polarization of damaged proteins during mitosis results in one cell that is relatively free of damage after division. In *Drosophila*, endogenous damaged proteins have been found to asymmetrically segregate in the female germline stem cell, intestinal stem cell and larval neuroblast *in vivo* (Bufalino et al., 2013). Htt aggregates have also been found to polarize during mitosis of embryonic neuroblasts in *Drosophila* (Rujano et al., 2006). In bacteria and yeast, the unequal inheritance of damaged proteins has been found to have a functional consequence, where the cell that receives the majority of

damaged proteins exhibits signs of aging (Lindner et al., 2008; Aguilaniu et al., 2003). Proteins destined for degradation also have been reported to asymmetrically segregate in mammalian cells *in vitro*; however, the effect of this phenomenon on cell fate has yet to be described (Fuentealba et al., 2008).

To determine the effect of diffuse Htt and inclusion bodies on proliferating cells, we studied the proliferation and resistance to stress of cancer cells expressing inducible Htt fused to GFP. We found that cells containing an inclusion body have reduced proliferation and increased resistance to stress compared to cells with diffuse Htt. Using live-imaging, we also demonstrate that cells inheriting the inclusion body during asymmetric division have an increased cell-cycle length and tendency to differentiate.

Materials and methods

Cell culture

14A2.5 cells were a kind gift from Leslie M. Thompson (Apostol et al., 2008) and maintained in Dulbecco's Modified Eagle Medium, high glucose (DMEM) supplemented with 10% horse serum, 5% fetal bovine serum, 200 μ g/mL Zeocin (Invitrogen), and 50 μ g/mL Geneticin (Gibco). Htt-GFP expression was induced by adding 10 μ M ponasterone A (Invitrogen) to the media for 24h, 4d after plating. Cells were grown at 37°C and 5% carbon dioxide.

Cell sorting

Cells were induced and counterstained with propidium iodide (0.9 μ L/mL, Invitrogen) prior to dissociation and sorting using a FACS Aria (BD Biosciences). The PulSA method (Ramdzan et al., 2012) was used to identify cells containing GFP aggregates, which can be differentiated from cells containing diffuse GFP based on a narrower and higher pulse shape.

Aggregate induction

14A2.5 cells were either exposed to maintenance media, 100 μ M of 2-BP (Sigma), 10 μ M of ponasterone A, or 10 μ M of ponasterone A and 100 μ M 2-BP 24h after plating. After 2d these cells were dissociated for experiments.

PrestoBlue assay

To assess viability and proliferation 100 μ L/mL of PrestoBlue (Invitrogen) was added to each well and cells were incubated for 1h in the dark at 37°C and 5% carbon dioxide. Fluorescence was measured using a SPECTRAmax GEMINI microplate spectrofluorometer (excitation 535nm, emission 615nm; Molecular Devices). The average fluorescence of wells containing media only were used to calculate background fluorescence and subtracted from values of wells with cells.

Cell proliferation

Proliferation of cells was measured at a population and single-cell level. Cells were induced and sorted into diffuse, inclusion body, and non-induced populations and plated at 350 cells/well in a 96-well Nunc plate. Proliferation was assessed using the PrestoBlue assay every day for 5d. Single cells were also plated in a 96-well Nunc plate and the number of cells was counted every day for 7d.

A similar procedure was used to assess proliferation of cells upon adding 2-BP. Cells in the induced, induced+2-BP, 2-BP, and non-induced conditions were plated at 350 cells/well of a 96-well plate and proliferation was assessed using the PrestoBlue assay every day for 5d.

Cell cycle length was estimated assuming exponential growth based on the following equation: $N(t) = C2^{t/d}$, where $N(t)$ is the relative fluorescence units of PrestoBlue or the number of cells on day 5, d is the doubling time, C is the relative fluorescence units of PrestoBlue or the number of cells on day 1, and t is time.

Immunocytochemistry

Cells were induced for 4d then plated in maintenance media for 24 h prior to staining. After washing in phosphate buffered saline (PBS), cells were fixed with 4% paraformaldehyde for 30 min at 4°C. Cells were rinsed three times in PBS, prior to blocking in 0.25% Triton X-100 PBS with 5% normal goat serum at 4°C overnight. Blocking solution was removed and cells were incubated with rabbit anti-activated

caspase 3 (1:200, abcam) in 0.25% Triton X-100 PBS with 1% normal goat serum overnight at 4°C. After three washes with 0.25% Triton X-100 PBS cells were incubated with goat anti-rabbit Alexa Fluor 568 for 3h at 4°C. Cells were washed three times with 0.25% Triton X-100 PBS prior to staining with Hoescht 33258 (1:1000, Sigma) for 10 min at room temperature. Images were captured at room temperature with the Olympus DP72 12.8 megapixel cooled digital color camera using a 10x (numerical aperture: 0.40) and 20x (numerical aperture: 0.45) objective of a confocal laser scanning microscope (FV1000, Olympus).

Stress exposure

Cells exposed to maintenance media, 2-BP, PA, or 2-BP and PA for 2d were dissociated and plated in maintenance media at 500 cells/well of a 96-well Nunc plate. After 24h, cells were exposed to DMSO control, 100 µM hydrogen peroxide (Sigma), or 300 nM doxorubicin hydrochloride (BioShop Canada Inc.). The PrestoBlue assay was used to measure cell viability 24h after treatment. Cells were imaged prior to treatment and 24h after treatment with the FV1000 Olympus confocal microscope described above.

Live-imaging

Time-lapse microscopy was performed using an automated Incucyte FLR microscope (Essen Bioscience) with a 10x objective (numerical aperture 1.49). Cells were induced for 4d and plated in BD Primaria tissue culture plates (BD Biosciences)

with maintenance media or differentiation media (DMEM high glucose, 1% horse serum, 0.5% fetal bovine serum, 200 μ g/mL Zeocin, 50 μ g/mL Geneticin, 50 ng/mL nerve growth factor (Invitrogen)) 4h prior to imaging. Phase-contrast and fluorescence images were captured for 9 fields of view of a 6-well plate every hour. Cell divisions were analyzed manually and ImageJ was used to measure neurite length.

Statistics

A two-way analysis of variance with Bonferroni posttests was used to analyze proliferation and stress exposure experiments. A two-tailed paired Student's *t*-test was used to compare the length of neurites on sister cells with and without an inclusion body.

Results and discussion

Cells containing an inclusion body have a longer cell-cycle than cells containing diffuse Htt

Developed from a rat pheochromocytoma cell line (PC12), 14A2.5 cells express a hybrid ecdysone receptor that allows for inducible expression of Htt containing 103 polyglutamine repeats fused to GFP (Apostol et al., 2003). After 4 days of induction with 10 μ M ponasterone A, 14A2.5 cells were sorted into populations of cells either containing an inclusion body or diffuse Htt (Figure 8A; method in Ramdzan et al., 2012).

Cells were plated in a 96-well plate at 350 cells/well and their proliferation was assessed over 5 days using the PrestoBlue assay. A two-way ANOVA demonstrated a significant interaction between cell population and time ($F(8,270) = 11.51, p < 0.05$) and Bonferroni posttests indicated that inclusion body cells had significantly lower proliferation than diffuse and non-induced cells on day 3-5 ($p < 0.05$). There was no significant difference between non-induced and diffuse cells at any time point ($p > 0.05$) (Figure 8B). The average doubling time for non-induced, diffuse, and inclusion body cells were 1.5, 1.6, and 3.0 days, respectively.

Proliferation was also measured after each population was sorted into plates with a single-cell per well. Consistent with the population study, diffuse and non-induced cells had significantly greater proliferation than inclusion body cells over 7 days (Figure 8D, examples in Figure 8C). Average doubling times were nearly identical when cells were plated 350 cells/well or as single cells per well, with times of 1.5, 1.6, and 2.8 days for non-induced, diffuse, and inclusion body single cells, respectively. A two-way ANOVA demonstrated a significant interaction between cell population and time ($F(12,483) = 2.78, p < 0.05$), and Bonferroni posttests indicated that all populations had significantly different cell numbers on Day 7, with inclusion body cells producing the fewest cells over 7 days ($p < 0.05$). Furthermore, only $7.1 \pm 2.7\%$ of the wells with inclusion body cells contained a single cell that divided at least once over a 7-day period, whereas the non-induced and inclusion body cells contained dividing cells in $19.0 \pm 3.6\%$ and $17.9 \pm 4.7\%$ of the wells, respectively. This may be an artifact due to the longer cell cycle time of inclusion body cells and/or cell death. When induced cells were stained for activated caspase 3 there were nearly double the number of inclusion body cells positive for this

indicator of apoptosis ($11.1 \pm 1.1\%$) compared to diffuse cells ($5.9 \pm 0.6\%$). Therefore, cells containing an inclusion body have reduced proliferation and increased cell death compared to cells containing diffuse Htt.

To control for the possibility that cell sorting preferentially changed the growth characteristics of inclusion body cells, proliferation also was assessed upon chemical induction of inclusion bodies in unsorted populations. 2-bromopalmitate (2-BP) reversibly inhibits palmitoylation, which is involved in trafficking Htt to the Golgi and has been shown previously to enhance the formation of inclusion bodies in Htt expressing cells (Yanai et al., 2006). When exposed to 2-BP during a 2d induction period, $73.4 \pm 2.2\%$ of cells contain inclusion bodies compared to $14.7 \pm 2.9\%$ of cells exposed to induction media only. This difference was also evident when cells were analyzed by FACS (Figure 9A). Analogous to the results of the sorted population growth curve, the population with the greatest number of inclusion bodies (induction + 2-BP) had the slowest doubling time at 2.5 days (Figure 9B). Adding 2-BP to non-induced cultures did not affect the growth rate compared to non-induced cells in growth media; average cell cycle times were 1.8 and 1.9 days, respectively. A two-way ANOVA demonstrated a significant interaction between cell population and time ($F(12,400) = 17.33, p < 0.05$), and Bonferroni posttests indicated that induced + 2-BP cells had significantly lower proliferation rates than diffuse and non-induced cells from Day 2-5 ($p < 0.05$).

Figure 8

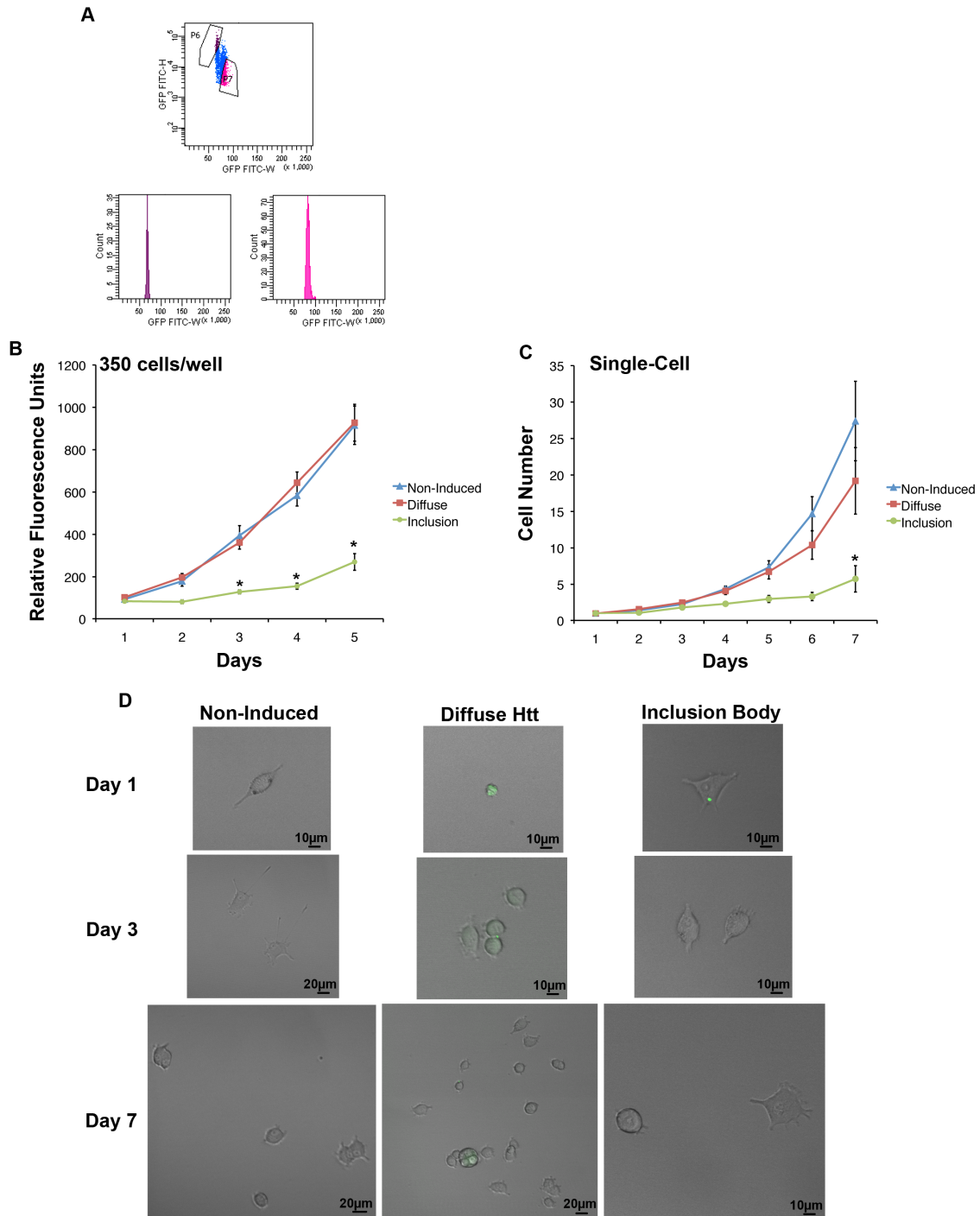


Figure 8. Inclusion body containing cells have a longer cell cycle than diffuse cells

(A) Htt-GFP expression was induced in 14A2.5 cells with 10 μ M of ponasterone-A for 4 days prior to cell suspension and sorting. Cells with inclusion bodies (population P6) can be sorted based on the GFP signal having a smaller height and width than cells containing diffuse GFP throughout the cell (population P7). (B) Live non-induced, diffuse, and inclusion body cells were sorted prior to plating at 350 cells/well in maintenance medium in a 96-well plate. The PrestoBlue viability assay was used to assess proliferation for 5d after plating. PrestoBlue is a resazurin-based compound that is converted into a fluorescent product upon reduction by a viable cell, increasing proportionally with cell number. The graph represents the average of three independent experiments and error bars indicate the standard error of the mean. Asterisks indicate a significant difference ($p < 0.01$) in proliferation between inclusion body cells and non-induced and diffuse cells by Bonferroni posttest. (C) Non-induced, diffuse and inclusion body cells were sorted into single cells per well of a 96-well plate. Cells were counted every day for 7d after plating. The graph represents the average of three independent experiments and error bars indicate the standard error of the mean. Asterisk indicates a significant difference ($p < 0.05$) in proliferation between inclusion body cells and non-induced and diffuse cells by Bonferroni posttest. (D) Examples of single-cell proliferation for non-induced (upper), diffuse (middle), and inclusion body cells (lower) (GFP is labeled in green).

Cells containing an inclusion body are more resistant to stress than cells with diffuse Htt

Currently, it is debated whether inclusion bodies cause the toxic effects of Htt or if they enhance a cell's ability to protect itself from stress (Arrasate & Finkbeiner, 2012). One hypothesis is that diffuse Htt is toxic because it disrupts proteasomal function and inclusion bodies reduce the amount of diffuse Htt within cells through aggregation thereby limiting their toxic effects (Arrasate & Finkbeiner, 2012). Due to the extensive differences in the diffuse and inclusion body populations, it was predicted that the response to stress would differ as well. When cells were exposed to oxidative stress (hydrogen peroxide) or Doxorubicin (a common chemotherapeutic that causes DNA damage) for 24h, the cells with the most inclusion bodies (induced + 2-BP) were more resistant than were non-induced and induced cells to both types of cell stress (Figure 9C, examples Figure 9D). A two-way ANOVA demonstrated significant main effects of treatment ($F(1,184) = 61.05, p < 0.05$) and cell population ($F(3,184) = 13.33, p < 0.05$). Bonferroni posttests indicated that adding 2-BP to growth medium did not significantly change the resistance of cells to either type of stress compared to non-induced cells ($p > 0.05$). Cells induced in the presence of 2-BP had a significantly greater ratio of viability (experiment:control) compared to non-induced and induced cells, indicating a protective effect of inclusion bodies ($p < 0.05$). Therefore, the most slowly cycling cells appear to be the most resistant to stress.

Figure 9

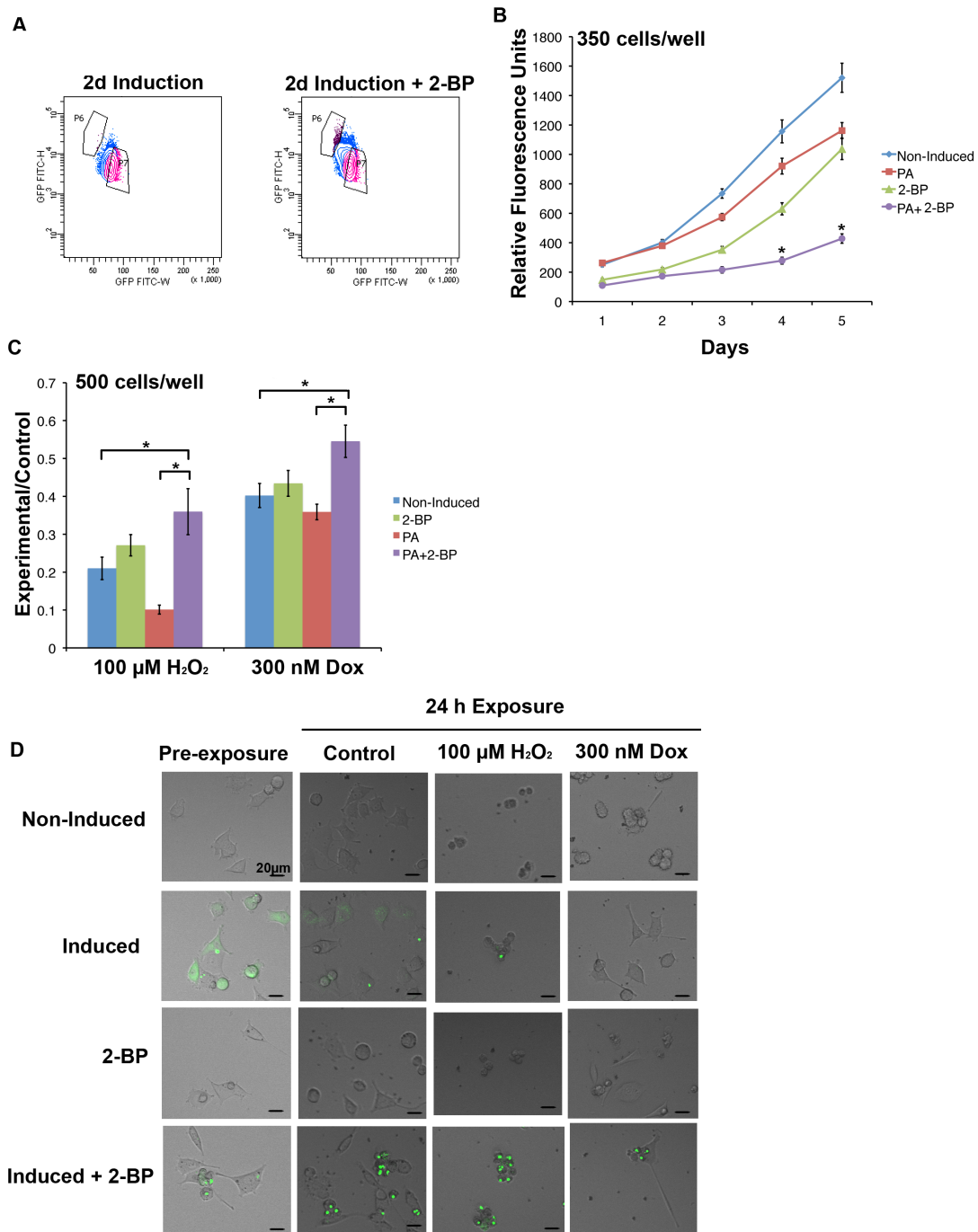


Figure 9. Increasing the number of inclusion body containing cells by inhibiting palmitoylation increases resistance to stress

(A) The population of cells induced in the presence of 2-BP for 2d has a distinct FACS profile from cells grown in induction medium, revealing an increase in the proportion of the population that contains inclusion bodies (population P6). (B) 14A2.5 cells were cultured in maintenance medium (non-induced), induction medium with and without 2-BP, and 2-BP in maintenance medium for 2d prior to plating at 350 cells/well in 96-well plates in maintenance medium. Cell viability was assessed every day for 5d after plating. The graph represents the average of three independent experiments error bars indicate the standard error of the mean. Asterisks indicate a significant difference ($p < 0.05$) in proliferation between cells in the induction + 2-BP condition compared to induced and non-induced cells by Bonferroni posttest. (C) To determine if inclusion bodies effect the ability of a cell to resist stress, the same cell populations were plated at 500 cells/well and treated after 24h of plating with hydrogen peroxide or doxorubicin for 24h. The PrestoBlue viability assay was used to compare cell viability of control and treated cells and the ratio of relative fluorescence units in each experimental condition to the same cell type in the maintenance condition is displayed on the y-axis. The graph represents an average of three independent experiments and error bars indicate the standard error of the mean. Asterisks indicate a significant difference ($p < 0.05$) in ratio of PrestoBlue in experiment:control conditions between cells in the induction + 2-BP condition compared to induced and non-induced cells by Bonferroni posttest. (D) Examples of cells in each condition prior to and following treatment (GFP is labeled in green).

Live-imaging reveals that asymmetric inheritance of inclusion bodies impacts cell fate

Of note, the number of differentiated cells differed between the diffuse and inclusion body cells. Neurite length is often used to measure the differentiation status of PC12 cells (Das et al., 2004), and only $0.8 \pm 0.4\%$ of cells induced for 2d had at least one neurite greater than $100\mu\text{m}$ in length, whereas $2.6 \pm 1.4\%$ of cells exposed to the induced + 2-BP condition for 2d consisted of these differentiated cells 1-2d after plating. Live-imaging was used to determine if the presence of an inclusion body influenced cell differentiation. When inclusion body containing cells were tracked by live imaging in growth media, no difference was seen in the morphology of the two daughter cells (one with an inclusion body and one without) immediately following division. However, there was a difference in the amount of time prior to the next division of the two daughter cells. In 81.2% of divisions tracked, the daughter cell containing the inclusion body did not divide or divided after the daughter cell without an inclusion body (Example Figure 10A). This lengthening of the cell cycle may be due to the time it takes to transport the inclusion body to an area of the cell where it will not interfere with cell division. It is interesting to note that aggregates of hepatitis B virus X protein have been found to lengthen the cell cycle (Song et al., 2003), in contrast to the non-aggregated protein that stimulates proliferation (Benn & Schneider, 1995). Therefore, the presence of an aggregate, regardless of the type of protein, may lengthen the cell cycle.

When inclusion body-containing cells were tracked while in differentiation media, there was a clear difference in morphology. In general, when at least one neurite of a cell reaches a length equal to or greater than the diameter of the cell body, the cell is

classified as differentiated (Das et al., 2004). After division of inclusion body containing cells, the daughter cells that received the inclusion body developed significantly longer neurites (average neurite length $109.3 \pm 19.9 \mu\text{m}$) than the daughter cells without an inclusion body (average neurite length $57.6 \pm 11.0 \mu\text{m}$) during imaging ($p < 0.05$ by paired two-tailed Student's t-test; example Figure 10B). Therefore, the presence of an inclusion body is associated with a longer cell-cycle and with enhanced differentiation.

How could an inclusion body influence multiple cell characteristics? We propose that each effect is mediated by a change in the activity of a single complex: the proteasome. Inclusion bodies and proteasome activity are intrinsically linked. Inclusion bodies decrease proteasome activity directly through sequestering components of the proteasome (Gil & Rego, 2008) and indirectly by overloading the capacity of the proteasome (Hipp et al., 2012). An inhibition of proteasome activity also increases the number of inclusion bodies in Htt expressing cells (Waelter et al., 2001). It is interesting to note that a common proteasome inhibitor, lactacystin, was initially characterized as a compound that blocked proliferation and promoted differentiation (Fenteany, 1998). Further studies discovered that proteasomal impairment prevents the degradation of factors involved in differentiation (Ito et al., 2011). This increases the amount of time that differentiation factors have to correctly localize and generate downstream effectors and is consistent with the cell-cycle length hypothesis that emphasizes the importance of longer cell cycle times for differentiation (Calegari & Huttner, 2003). On the other hand, proliferation depends on the degradation of proteins throughout the cell cycle. For example, Cyclin B promotes the G2-M transition and its degradation is required for the

cell to exit mitosis (Reed, 2003). Therefore, cells containing an inclusion body may have enhanced differentiation and reduced proliferation due to proteasomal impairment.

The increased cell cycle length of cells with an inclusion body may also explain their increased resistance to oxidative stress compared to cells with diffuse Htt. A longer cell cycle has been associated with reduced general energy metabolism (Alida et al., 2010) and therefore reduced levels of intracellular ROS, a common by-product of metabolism. Although a population of inclusion body containing cells is more resistant to extreme stress than a population of cells with diffuse Htt, the small percentage of cells in apoptosis under maintenance conditions was greater in cells containing inclusion bodies. This discrepancy with a previous study that found an association between cell death and high levels of diffuse Htt, but not inclusion body presence, in neurons (Arrasate et al., 2004), can be explained by the ability of cells to undergo division in the present study. In maintenance conditions, cells with diffuse Htt rapidly proliferate, which dilutes the level of Htt and any other damaged cellular components. Although the presence of an inclusion body decreases the level of diffuse Htt within cells, their slower rate of cell division prevents them from diluting any toxic by-products of diffuse Htt exposure that may have accumulated before the inclusion body formed, thus leading to higher rates of cell death for proliferating cells with inclusion bodies compared to diffuse Htt. For example, the level of a toxic product of lipid peroxidation, 4-hydroxy-2-nonenal, has been found to increase in the presence of Htt and its accumulation may be responsible for increased cell death in inclusion body containing cells (Lee et al., 2011).

Conclusions

Overall, cells containing Htt in a diffuse and inclusion body form are distinct in terms of proliferation, death, resistance to stress and differentiation. In future studies, it would be interesting to explore the level of proteasome activity in cells with an inclusion body and diffuse Htt to determine if inclusion body-dependent proteasome inhibition is responsible for the decreased proliferation and enhanced differentiation of inclusion body containing cells. We predict that enhancing proteasome activity in cells with an inclusion body would increase proliferation.

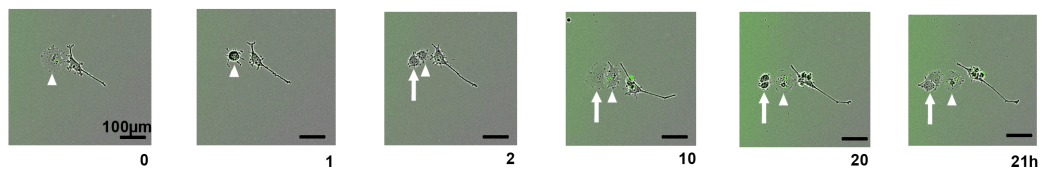
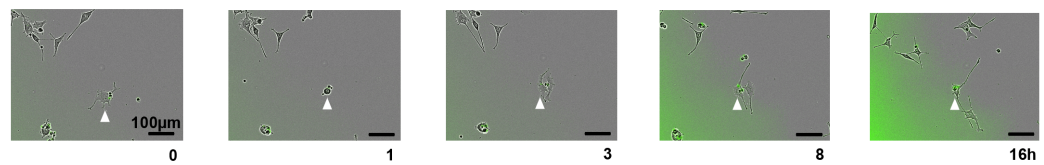
Figure 10**A Growth Medium****B Differentiation Medium**

Figure 10. Live-imaging reveals differences in cell-fate of asymmetrically dividing inclusion body cell progeny

(A) Example of an inclusion body cell (arrowhead) in maintenance medium that undergoes cell division (GFP is labeled in green). The progeny that does not inherit the inclusion body (arrow) divides before the cell that received the inclusion body (arrowhead) (n = 16). (B) Example of an inclusion body cell (arrowhead) in differentiation medium that undergoes cell division (GFP is labeled in green). Neurite length is longer in the cell that inherits the inclusion body (n = 15).

CHAPTER 4

General Discussion

In this thesis, I have shown that the asymmetric segregation of damaged proteins is conserved in stem cells *in vivo* and has functional consequences when cells are tracked *in vitro* using live-imaging. Using *Drosophila* as a model system, I demonstrated that the asymmetric division of damaged proteins is a common feature of stem cells, but that not all stem cells segregate damage to the same cell type. Furthermore, both extrinsic and intrinsic factors were found to mediate the polarization of damaged proteins within stem cells (Chapter 2). I also found that the structural conformation of damaged proteins determines its impact on proliferating cells using a cancer cell line expressing Htt-GFP. Cancer cell proliferation was impaired only when damaged proteins were in an aggregated form and this aggregation also increased the resistance of cells to oxidative stress. Live-imaging revealed that inheritance of an Htt aggregate during mitosis increased cell-cycle length and differentiation (Chapter 3).

Functional significance of asymmetric damaged protein inheritance *in vivo*

An unequal distribution of damaged proteins during mitosis was found in all three stem cell populations, indicating that the segregation of factors associated with age is conserved across developmental stages (larval and adult) and stem cell types (germline and somatic). Conserved asymmetric division of damaged proteins can give stem cells a defense against one major cause of aging, the build-up of molecules damaged by reactive oxygen species (Giorgio et al., 2007); however, both the GSC and NB retain damage at division. In all three stem cell populations the division is asymmetric with respect to cell fate, lifespan, mitotic activity, and damaged proteins. Both the fate of the cell

(undifferentiated vs. differentiated) and its mitotic activity do not correlate with damaged protein asymmetry. For example, both NBs and ISCs are more mitotically active than their differentiating progeny (GMC and enteroblast, respectively), yet they showed opposite patterns of damaged protein localization. In contrast, cell lifespan can predict the cell type that will receive the majority of damaged proteins at division.

The NB, which retains damaged proteins at division, undergoes apoptosis or differentiates into unknown cells types during pupation making it shorter-lived than its neuronal progeny, which persist to adulthood (Chell and Brand, 2008). The GSC also retains damaged proteins and is shorter-lived than its cystoblast progeny, because the cystoblast can form a new organism with the ability to outlive the mother where the GSC resides. This is distinct from ISCs, which are present throughout the organisms lifespan and segregate damaged proteins towards differentiating progeny, that are replaced approximately every week (Micchelli and Perrimon, 2006; Ohlstein and Spradling, 2006). Therefore, the difference in functional lifespan between sister cells is able to predict the cell that will receive the majority of damaged proteins during asymmetric division. This is consistent with the field of centrosome inheritance where lifespan may also be able to predict which cell inherits the mother centrosome. Historically, the mother centrosome was consistently found to associate with the stem cell during asymmetric division; however, the larval NB retains the daughter centrosome leading to the hypothesis that lifespan, and not stemness, can predict the cell that inherits the mother centrosome (Januschke et al., 2011).

The asymmetric division of damaged proteins may function to prevent the longer-lived cells from accumulating these factors, thus maintaining them in a younger more

viable state. The finding that ISCs show a greater resistance to the accumulation of damaged proteins with age compared to GSCs and segregate damage to differentiating progeny, suggests that HNE asymmetry does have a protective role for longer-lived progeny. This is consistent with the finding in yeast, that an uneven distribution of cellular components involved in aging (DNA circles) has a protective effect for the bud cell, which receives fewer DNA circles and can divide more times than the mother cell (Shcheprova et al., 2008). Asymmetric division of damaged proteins has not been shown in adult mammalian stem cells *in vivo*. It is interesting to note, however, that mammalian stem cells can be induced to proliferate when they contain high levels of ROS (Jang & Sharkis, 2007; Le Belle et al., 2011). The activation of signaling pathways involved in proliferation by increased levels of ROS may also serve as a protective mechanism for long-lived stem cells to get rid of damaged proteins through cell division before they reach a toxic level in the cell.

Potential mechanisms of damaged protein polarization

The mechanism(s) of this unequal damage division in stem cells is an interesting area for future study. The stem cell niche was found to be involved based on the association of areas rich in protein damage with DE-Cadherin, a component of adherens junctions, and the abolishment of HNE asymmetry with mechanical and genetic alterations of the NB niche. DE-Cadherin has important roles in the niche of all three stem cell systems (Song et al., 2002; Dumstrei et al., 2003; Maeda et al., 2008). DE-Cadherin has also been found to be essential for correct centrosome orientation in

Drosophila male GSCs (Inaba et al., 2010). The role of Cadherin-mediated cell-cell adhesion in establishing polarity is a conserved mechanism, as it is also sufficient to induce centrosome orientation and direction of migration in a mammalian cell line (Desai et al., 2009). There is also evidence that cell-cell contact is involved in the asymmetric segregation of template DNA. Under normal conditions a small percentage of cancer cells *in vitro* display asymmetric DNA segregation; however, this is abolished when single cancer cells are cultured with a membrane preventing cell-cell contact, but permeable to diffusible factors (Pine et al., 2010).

Despite the important role of the niche in damaged protein segregation, the finding that asymmetry develops during the NB cell cycle when the NB is mechanically dissociated from its niche and cultured *in vitro*, suggests that additional mechanisms exist to polarize damaged proteins. One candidate is the polarisome, a site for actin polymerization in the yeast bud tip that extends actin cables into the mother cell along which damaged proteins are transported from the bud to the mother (Moseley & Goode, 2006; Liu et al., 2010). When the polarisome is disrupted through mutations in its components, replicative lifespan of yeast is shortened indicating that this mechanism is essential for clearing damaged proteins from the bud cell (Liu et al., 2010). So far, a similar mechanism has not been reported in multi-cellular organisms. An alternative strategy to create different levels of damaged protein within regions of a cell is to enhance the degradation of damaged proteins on one side of the cell. Although this has not been tested directly, proteasomal activity has been found to increase when embryonic stem cells differentiate (Hernebring et al., 2006). One type of damaged protein, advanced glycation end products, was reduced to less than half that of baseline levels after 12 h of

differentiation (Hernebring et al., 2006). An earlier time point was not reported; however, it is possible that degradation activity is enhanced even as polarity is established in a dividing cell and this presents an interesting area for future study.

In yeast, it has been argued that no mechanism is required to segregate damaged proteins to the mother cell (Zhou et al., 2011). By tracking protein aggregates during live-imaging, the movement of protein aggregates during mitosis was found to be random and disrupting the actin cytoskeleton did not prevent the accumulation of damaged proteins in the mother cell (Zhou et al., 2011). The authors proposed that aggregates have limited mobility, which prevents them from entering the bud cell through the narrow bud neck during the short period of mitosis (Zhou et al., 2011). Similar to yeast, the asymmetric division of the *Drosophila* larval NB results in the accumulation of damaged proteins in the much larger NB instead of the smaller GMC. Still it is likely that a localization mechanism to retain damaged proteins in the NB exists, because in cell size mutants where the NB and GMC are similar sizes, there is still significantly greater accumulation of damaged proteins in the NB (Chapter 2).

Advantages of asymmetric damaged protein division

In multi-cellular organisms where cell division must remain balanced with cell death, the asymmetric division of damaged proteins provides a convenient method to produce “young” cells. In contrast, cells without the need for growth restraint would not require a mechanism to asymmetrically segregate damage that they could instead dilute through cell division. It has been argued that cells able to continuously divide

symmetrically have an unlimited lifespan (Gladyshev, 2012). If a cell is able to live forever by diluting damage through cell division before it reaches a toxic level, why did mechanisms for the asymmetric division of damaged proteins arise during evolution? Cells in a stressful environment may be at a disadvantage if divisions are completely symmetric. For example, if a cell experiences a high level of stress there are two possible outcomes: 1) asymmetric division resulting in one cell with a low and one with a high level of stress; 2) symmetric division resulting in two cells with a medium level of stress. In a scenario where a second stressful event occurs immediately following cell division, the cell that underwent asymmetric division is more likely to survive, because stress will reach a toxic level in all cells except for the one with a low level of damage. Therefore, asymmetric division may be advantageous even in cells with rapid proliferation.

The ability to switch between asymmetric and symmetric division may provide the greatest survival benefit, as it would result in a diverse population of cells. Asymmetric division alone, although most protective of repeated stress, results in one cell with a high level of damage that may reduce its ability to divide. In this situation, only one cell is able to proliferate rapidly and the rate of population growth would be reduced compared to symmetrically dividing cells. One of the best examples of the survival benefits of a heterogeneous population is cancer. By containing cells that proliferate at different rates, a portion of the population can escape the toxic effects of chemotherapies that target rapidly proliferating cells and repopulate the tumor when the environment improves.

Tumor heterogeneity has been described in many tissues. For example, both melanoma and non-small cell lung cancer cells contain a sub-population of cells *in vitro*

that have reduced proliferation, and this sub-population in non-small cell lung cancer cells is resistant to chemotherapy (Roesch et al., 2010; Sharma et al., 2010). Breast tumors *in vivo* and *in vitro* also contain a sub-population of cells that are slowly proliferating (Diehn et al., 2009; Dey-Guha et al., 2011). These tumors consist of both proliferating and non-tumorigenic cells, which were found to differ in ROS content. Proliferating cells contain lower ROS levels than non-tumorigenic cells and are more resistant to treatment (Diehn et al., 2009). The difference in ROS content was suggested to be due to enhanced ROS scavenging systems in proliferating cells (Diehn et al., 2009); however, it is also possible that asymmetric division contributed to this difference as the behaviour of ROS and damaged proteins during cell division was not reported. It is interesting to note that breast cancer cells are able to switch from an asymmetric to symmetric mode of division and vice-versa, allowing them to respond quickly to changes in the environment (Dey-Guha et al., 2011).

The cellular heterogeneity of tumors that prevents cancer elimination during chemotherapy could also be exploited to slow cancer progression. Asymmetric division is suppressed in advanced stages of colon cancer (Gu et al., 2013); therefore, it may be possible to slow the progression of cancer (both tumor growth and metastasis) by enhancing asymmetric division. Although mechanisms of asymmetric division have been reported for some types of cancer and include well-known cell fate determinates, treatments that target these pathways will only be effective as long as these pathways are not mutated. For example, micro-RNA (miR-34a) regulates asymmetric division in colon cancer by generating a polarized distribution of Notch, but it is suppressed in advanced stages of cancer (Gu et al., 2013). An ideal treatment would slow cancer cell proliferation

and force cells to divide asymmetrically without being dependent on a classical polarity system.

Cancer treatments that induce protein aggregation

In this thesis, the segregation of damaged proteins to inclusion bodies was found to reduce cell proliferation and result in asymmetric division. Although the possibility that cell fate determinants were affected by inclusion bodies has not been ruled out, it is more likely that protein aggregates, with their large size and associated toxicity, would interfere with the polarity machinery than specifically promote the polarization of cell fate determinants. Therefore, increasing the formation of inclusion bodies in cancer cells may be one strategy to slow the progression of cancer. Many studies have examined the toxicity of agents that increase the amount of damaged proteins in cancer cells. For example Bortezomib, a reversible proteasome inhibitor approved for use in cancer treatment, increases the generation of ROS and inclusion bodies (Ling et al., 2003; Catley et al., 2006). Bortezomib reduces proliferation and increases the sensitivity of cancer cells to radiation and chemotherapy (Ludwig et al., 2005). It is interesting to note that inhibiting inclusion body formation can increase the effectiveness of Bortezomib (Catley et al., 2006; Nawrocki et al., 2006). This is due to the protective role of inclusion bodies. When abnormal proteins are segregated into a large aggregate the efficiency of their removal through autophagy is increased and the level of damaged proteins within a cell is reduced (Kopito, 2000).

Although Bortezomib causes toxicity through multiple pathways (Chen et al., 2011), the involvement of ROS raises the possibility that cancer cells could evade

Bortezomib toxicity through cell division. If the presence of an inclusion body is linked to reduced proliferation in Bortezomib treated cells, combining agents that reduce inclusion body formation with Bortezomib may even increase the ability of cells to dilute damage through cell division and evade cell death. An alternate approach would be to induce the formation of inclusion bodies with Bortezomib and prevent their elimination through autophagy. Inhibitors of autophagy have been shown to sensitize cancer cells to the effects of a wide range of chemotherapeutics when used in combination (Yang et al., 2011). When bortezomib and an inhibitor of autophagy (chloroquine) treatments are combined, their suppression of tumor growth is greater than when either treatment is used alone (Ding et al., 2009). This study did not examine the mode of cancer cell division (symmetric/asymmetric) or the role of inclusion bodies in tumor growth suppression. Based on the results presented in this thesis, it is predicted that in this combination treatment there is an increased percentage of cancer cells containing inclusion bodies, which forces cells to divide asymmetrically and reduces cell proliferation.

Theories on the role of inclusion bodies in cell fate decisions

The relationship between proteasome inhibition and the generation of inclusion bodies is not one-sided. Just as proteasome inhibition leads to inclusion body production, there is increasing evidence that the presence of an inclusion body leads to decreased proteasome function. Inclusion bodies sequester many normal proteins, especially those related to reducing the level of damaged proteins within a cell. For example, heat shock proteins involved in refolding misfolded proteins and components of the proteasome are

sequestered by inclusion bodies (Gil & Rego, 2008). Even the sequestering of chaperone proteins alone may be sufficient to impair proteasomal function. When chaperones are recruited to inclusion bodies, they are unavailable to refold other misfolded proteins. This increases the number of damaged proteins that must now be degraded through the proteasome, overwhelming its capacity (Hipp et al., 2012).

Proteasome inhibition may explain the impact of inclusion bodies on cell fate. Similar to cells with an inclusion body, cells with decreased proteasome activity have reduced proliferation and enhanced differentiation (Fenteany, 1998). For a cell to undergo mitosis, many proteins need to be active only during a distinct window of time and are rapidly degraded by the proteasome when their function is no longer required. For example, to initiate DNA replication Sic1 must be degraded and to exit mitosis Cyclin B must be degraded (Reed, 2003). Therefore, inclusion bodies may increase cell-cycle length by reducing proteasome activity. An increased cell-cycle length and reduced degradation of differentiation promoting factors may be responsible for the enhanced differentiation seen when proteasome activity is inhibited. The cell-cycle length hypothesis proposes that the length of the cell-cycle influences the ability of cell fate determinants to act because they need time to be produced, correctly localize and/or generate any downstream effectors (Calegari & Huttner, 2003). However, increasing cell-cycle length will not have an effect on differentiation if differentiation signals and downstream effectors are rapidly degraded. Decreasing proteasome activity also exposes a cell to the effects of a differentiation factor for a longer period of time. For example, the level of phosphorylated Smad is higher in myoblasts that have been exposed to the proteasome inhibitor lactacystin, which was linked to enhanced differentiation of

myoblasts to osteoblasts *in vitro* (Ito et al., 2011). Therefore, inclusion bodies may impact proliferation and differentiation of a cell by decreasing proteasome activity.

Conclusions

The ubiquitous presence of damaged proteins in cells highlights the importance of increasing our understanding of how cells manage damaged proteins and are influenced by them. In this thesis, I confirmed that the asymmetric segregation of damaged proteins is conserved in non-diseased cells *in vivo* across developmental stages (larval and adult) and tissue types (germline and somatic). Future studies in mammalian models of long-lived stem cell populations are expected to find that these stem cells segregate damaged proteins to differentiating progeny. I also revealed that the structural conformation of damaged proteins directs cell fate in mammalian cells, as aggregates increased cell-cycle length and differentiation. An aggregate dependent reduction of proteasome activity was proposed to be responsible for the fate of cells containing an aggregate. Future studies are predicted to confirm that proteasome activity is reduced in cells with aggregates and that increasing proteasome activity in cells with aggregates can increase their proliferation. These results can be used to explain the effectiveness of cancer treatments employing drugs that inhibit the proteasome and autophagy, which are predicted to act through increasing damaged protein aggregation and asymmetric division. If this is the case, novel treatments based on the most effective method to increase the production and retention of protein aggregates in cancer cells could be designed to further improve the outcome of cancer patients.

REFERENCE LIST

- Aguilaniu, H., L. Gustafsson, M. Rigoulet, T. Nyström. 2003. Asymmetric inheritance of oxidatively damaged proteins during cytokinesis. *Science*. 299:1751-1753.
- Alida, M., G. Essers, A. Trumpp. 2010. Targeting leukemic stem cells by breaking their dormancy. *Molecular Oncology*. 4:443-450.
- Apostol, B.L., D.A. Simmons, C. Zuccato, et al.. 2003. A cell-based assay for aggregation inhibitors as therapeutics of polyglutamine-repeat disease and validation in *Drosophila*. *Proc. Natl. Acad. Sci. USA*. 100:5950-5.
- Arrasate, M., S. Finkbeiner. 2012. Protein aggregates in Huntington's disease. *Experimental Neurology*. 238:1-11.
- Arrasate, M., S. Mitra, E.S. Schweitzer, M.R. Segal, S. Finkbeiner. 2004. Inclusion body formation reduces levels of mutant huntingtin and the risk of neuronal death. *Nature*. 431:805-10.
- Barrera, G. 2012. Oxidative stress and lipid peroxidation products in cancer progression and therapy. *ISRN Oncol*. 2012:137289.
- Bello, B.C., N. Izergina, E. Caussinus, H. Reichert. 2008. Amplification of neural stem cell proliferation by intermediate progenitor cells in *Drosophila* brain development. *Neural development*. 3:5.
- Benn, J., R.J. Schneider. 1995. Hepatitis B virus HBx protein deregulates cell cycle checkpoint controls. *Proc. Natl. Acad. Sci. USA*. 92:11215-9.
- Boone, J.Q., C.Q. Doe. 2008. Identification of *Drosophila* type II neuroblast lineages containing transit amplifying ganglion mother cells. *Dev Neurobiol*. 68:1185-95.
- Brys, K., J.R. Vanfleteren, B.P. Braeckman. 2007. Testing the rate-of-living/oxidative damage theory of aging in the nematode model *Caenorhabditis elegans*. *Exp. Gerontol*. 42:845-51.
- Bu, P., K.-Y. Chen, J.H. Chen, et al.. 2013. A microRNA miR-34a-Regulated Bimodal Switch Targets Notch in Colon Cancer Stem Cells. *Cell Stem Cell*. 12:602-615.
- Bufalino, M. R., B.D. Deveale, D. van der Kooy. 2013. The asymmetric segregation of damaged proteins is stem cell-type dependent. *J. Cell Biol*. 201:523-30.
- Bussard, K.M., C.A. Boulanger, F.S. Kittrell, F. Behbod, D. Medina, G. H. Smith. 2010. Immortalized, pre-malignant epithelial cell populations contain long-lived, label-retaining cells that asymmetrically divide and retain their template DNA. *Breast Cancer Res*. 12:R86.
- Butterfield, D.A., T. Reed, R. Sultana. 2011. Roles of 3-nitrotyrosine- and 4-hydroxynonenal-modified brain proteins in the progression and pathogenesis of Alzheimer's disease. *Free. Radic. Res*. 45:59-72.
- Calegari, F., W.B. Huttner. 2003. An inhibition of cyclin-dependent kinases that lengthens, but does not arrest, neuroepithelial cell cycle induces premature neurogenesis. *J. Cell. Sci*. 116:4947-55.

- Catley, L., E. Weisberg, T. Kiziltepe, et al.. 2006. Aggresome induction by proteasome inhibitor bortezomib and α -tubulin hyperacetylation by tubulin deacetylase (TDAC) inhibitor LBH589 are synergistic in myeloma cells. *Blood*. 108:3441-3449.
- Chell, J.M., A.H. Brand. 2008. Forever young: death-defying neuroblasts. *Cell*. 133:769-771.
- Chen, D., M. Frezza, S. Schmitt, J. Kanwar, Q.P. Dou. 2011. Bortezomib as the first proteasome inhibitor anticancer drug: current status and future perspectives. *Curr. Cancer Drug Targets*. 11:239-53.
- Choi, J., S. Artandi. 2009. Stem cell aging and aberrant differentiation within the niche. *Cell Stem Cell*. 5:6-8.
- Clague, M.J., S. Urbé. 2010. Ubiquitin: same molecule, different degradation pathways. *Cell*. 143:682-5.
- Clarke, M.F., M. Fuller. 2006. Stem cells and cancer: two faces of eve. *Cell*. 124:1111-5.
- Cohen, A., L. Ross, I. Nachman, S. Bar-Nun. 2012. Aggregation of PolyQ Proteins Is Increased upon Yeast Aging and Affected by Sir2 and Hsf1: Novel Quantitative Biochemical and Microscopic Assays. *PLoS ONE*. 7:e44785.
- Das, J., S. Kar, R. Liu, et al.. 2004. Assessment of PC12 cell differentiation and neurite growth: a comparison of morphological and neurochemical measures. *Neurotoxicol. Teratol*. 26:397-406.
- Demontis, F., N. Perrimon. 2010. FOXO/4E-BP signaling in Drosophila muscles regulates organism-wide proteostasis during aging. *Cell*. 143:813-825.
- Deng, W., H. Lin. 1997. Spectrosomes and fusomes anchor mitotic spindles during asymmetric germ cell divisions and facilitate the formation of a polarized microtubule array for oocyte specification in Drosophila. *Dev. Biol*. 189:79-94.
- Desai, R.A., L. Gao, S. Raghavan, W.F. Liu, C.S. Chen. 2009. Cell polarity triggered by cell-cell adhesion via E-cadherin. *J. Cell Sci*. 122:905-11.
- Dey-Guha, I., A. Wolfer, A.C. Yeh, et al.. 2011. Asymmetric cancer cell division regulated by AKT. *Proc. Natl. Acad. Sci. USA*. 108:12845-50.
- Diehn, M., R.W. Cho, N.A. Lobo, et al.. 2009. Association of reactive oxygen species levels and radioresistance in cancer stem cells. *Nature*. 458:780-3.
- Ding, W.-X., H.-M. Ni, W. Gao, et al.. 2009. Oncogenic transformation confers a selective susceptibility to the combined suppression of the proteasome and autophagy. *Mol. Cancer Ther*. 8:2036-2045.
- Dumstrei, K., F. Wang, V. Hartenstein. 2003. Role of DE-cadherin in neuroblast proliferation, neural morphogenesis, and axon tract formation in Drosophila larval brain development. *J. Neurosci*. 23:3325-3335.
- Fenteany, G. 1998. Lactacystin, Proteasome Function, and Cell Fate. *Journal of Biological Chemistry*. 273:8545-8548.
- Finkel, T., N.J. Holbrook. 2000. Oxidants, oxidative stress and the biology of ageing. *Nature*. 408:239-47.
- Friguet, B., L.I. Szweda. 1997. Inhibition of the multicatalytic proteinase (proteasome) by 4-hydroxy-2-nonenal cross-linked protein. *FEBS. Lett*. 405:21-25.

- Fuentealba, L.C., E. Eivers, D. Geissert, et al.. 2008. Asymmetric mitosis: Unequal segregation of proteins destined for degradation. *Proc. Natl. Acad. Sci. USA*. 105:7732-7737.
- Fuller, M.T., A.C. Spradling. 2007. Male and female Drosophila germline stem cells: two versions of immortality. *Science*. 316:402-404.
- Furriols, M., S. Bray. 2001. A model Notch response element detects Suppressor of Hairless-dependent molecular switch. *Curr. Biol*. 11:60-64.
- Gil, J.M., A.C. Rego. 2008. Mechanisms of neurodegeneration in Huntington's disease. *European Journal of Neuroscience*. 27:2803-2820.
- Gilbertson, R.J., J.N. Rich. 2007. Making a tumour's bed: glioblastoma stem cells and the vascular niche. *Nat. Rev. Cancer*. 7:733-6.
- Gilbertson, R.J., T.A. Graham. 2012. Cancer: Resolving the stem-cell debate. *Nature*. 488:462-3.
- Giorgio, M., M. Trinei, E. Migliaccio, P.G. Pelicci. 2007. Hydrogen peroxide: a metabolic by-product or a common mediator of ageing signals? *Nat. Rev. Mol. Cell Biol*. 8:722-728.
- Gladyshev, V.N. 2012. On the cause of aging and control of lifespan. *Bioessays*. 34:925-929.
- Goulas, S., R. Conder, J.A. Knoblich. 2012. The Par Complex and Integrins Direct Asymmetric Cell Division in Adult Intestinal Stem Cells. *Cell Stem Cell*. 11:529-540.
- Greene, L.A., A.S. Tischler. 1976. Establishment of a noradrenergic clonal line of rat adrenal pheochromocytoma cells which respond to nerve growth factor. *Proc. Natl. Acad. Sci. USA*. 73:2424-8.
- Grune, T., T. Jung, K. Merker, K.J.A. Davies. 2004. Decreased proteolysis caused by protein aggregates, inclusion bodies, plaques, lipofuscin, ceroid, and 'aggresomes' during oxidative stress, aging, and disease. *Int. J. Biochem. Cell Biol*. 36:2519-30.
- Gupta, S.C., D. Hevia, S. Patchva, et al.. 2012. Upsides and downsides of reactive oxygen species for cancer: the roles of reactive oxygen species in tumorigenesis, prevention, and therapy. *Antioxid. Redox. Signal*. 16:1295-322.
- Gutkunst, C.A., S.H. Li, H. Yi, et al.. 1999. Nuclear and neuropil aggregates in Huntington's disease: relationship to neuropathology. *J. Neurosci*. 19:2522-34.
- Harman D. 1956. Aging: A theory based on free radical and radiation chemistry. *J. Gerontol*. 11:298-300.
- Hipp, M.S., N. Patel, K. Bersuker, et al.. 2012. Indirect inhibition of 26S proteasome activity in a cellular model of Huntington's disease. *J. Cell Biol*. 196:573-587.
- Horvitz, H.R., I. Herskowitz. 1992. Mechanisms of asymmetric cell division: two Bs or not two Bs, that is the question. *Cell*. 68:237-55.
- Hour, T.-C., C.-Y. Huang, C.-C. Lin, et al.. 2004. Characterization of molecular events in a series of bladder urothelial carcinoma cell lines with progressive resistance to arsenic trioxide. *Anticancer Drugs*. 15:779-85.
- Inaba, M., H. Yuan, V. Salzmann, et al.. 2010. E-cadherin is required for centrosome and spindle orientation in Drosophila male germline stem cells. *PLoS. One*. 5:, e12473.

- Inaba, M., Y.M. Yamashita. 2012. Asymmetric Stem Cell Division: Precision for Robustness. *Cell Stem Cell*. 11:461-469.
- Ishimoto, T., O. Nagano, T. Yae, et al.. 2011. CD44 variant regulates redox status in cancer cells by stabilizing the xCT subunit of system xc(-) and thereby promotes tumor growth. *Cancer Cell*. 19:387-400.
- Ito, Y., H. Fukushima, T. Katagiri, et al.. 2011. Lactacystin, a proteasome inhibitor, enhances BMP-induced osteoblastic differentiation by increasing active Smads. *Biochem. Biophys. Res. Commun.* 407:225-229.
- Izumi, H., Y. Kaneko. 2012. Evidence of asymmetric cell division and centrosome inheritance in human neuroblastoma cells. *Proc. Natl. Acad. Sci. USA*. 109:18048-18053.
- Jang, Y.-Y., S.J. Sharkis. 2007. A low level of reactive oxygen species selects for primitive hematopoietic stem cells that may reside in the low-oxygenic niche. *Blood*. 110:3056-63.
- Januschke, J., S. Llamazares, J. Reina, C. Gonzalez. 2011. Drosophila neuroblasts retain the daughter centrosome. *Nat. Commun.* 2:243-8.
- Karpowicz, P., C. Morshead, A. Kam, et al.. 2005. Support for the immortal strand hypothesis: neural stem cells partition DNA asymmetrically in vitro. *J. Cell Biol.* 170:721-32.
- Karpowicz, P., M. Pellikka, E. Chea, et al.. 2009. The germline stem cells of Drosophila melanogaster partition DNA non-randomly. *Eur. J. Cell Biol.* 88:397-408.
- Kirilly, D., T. Xie. 2007. The Drosophila ovary: an active stem cell community. *Cell Res.* 17:15-25.
- Knoblich, J.A. 2008. Mechanisms of asymmetric stem cell division. *Cell*. 132:583-97.
- Kopito, R.R. 2000. Aggresomes, inclusion bodies and protein aggregation. *Trends Cell Biol.* 10:524-30.
- Kruegel, U., B. Robison, T. Dange, et al.. 2011. Elevated proteasome capacity extends replicative lifespan in Saccharomyces cerevisiae. *PLoS Genet.* 7:e1002253.
- Kuemmerle, S., C.A. Gutekunst, A.M. Klein, et al.. 1999. Huntington aggregates may not predict neuronal death in Huntington's disease. *Ann. Neurol.* 46:842-9.
- Lambert, J.D., L.M. Nagy. 2002. Asymmetric inheritance of centrosomally localized mRNAs during embryonic cleavages. *Nature*. 420:682-6.
- Lansdorp, P.M. 2007. Immortal strands? Give me a break. *Cell*. 129:1244-7.
- Lathia, J.D., M. Hitomi, J. Gallagher, et al.. 2011. Distribution of CD133 reveals glioma stem cells self-renew through symmetric and asymmetric cell divisions. *Cell Death and Disease*. 2:e200-11.
- Le Belle, J.E., N.M. Orozco, A.A. Paucar, et al.. 2011. Proliferative Neural Stem Cells Have High Endogenous ROS Levels that Regulate Self-Renewal and Neurogenesis in a PI3K/Akt-Dependant Manner. *Cell Stem Cell*. 8:59-71.
- Lee, J., B. Kosaras, S. J. Del Signore, et al. 2011.. Modulation of lipid peroxidation and mitochondrial function improves neuropathology in Huntington's disease mice. *Acta Neuropathol.* 121:487-498.

- Lenehan, P.F., P.L. Gutierrez, J.L. Wagner, et al.. 1995. Resistance to oxidants associated with elevated catalase activity in HL-60 leukemia cells that overexpress multidrug-resistance protein does not contribute to the resistance to daunorubicin manifested by these cells. *Cancer Chemother. Pharmacol.* 35:377-86.
- Lin, H., L. Yue, A.C. Spradling. 1994. The Drosophila fusome, a germline-specific organelle, contains membrane skeletal proteins and functions in cyst formation. *Development.* 120:947-956.
- Lindner, A.B., R. Madden, A. Demarez, et al. 2008. Asymmetric segregation of protein aggregates is associated with cellular aging and rejuvenation. *Proc. Natl. Acad. Sci. USA.* 105:3076-3081.
- Ling, Y.-H., L. Liebes, Y. Zhou, R. Perez-Soler. 2003. Reactive Oxygen Species Generation and Mitochondrial Dysfunction in the Apoptotic Response to Bortezomib, a Novel Proteasome Inhibitor, in Human H460 Non-small Cell Lung Cancer Cells. *Journal of Biological Chemistry.* 278:33714-33723.
- Liu, B., L. Larsson, A. Caballero, et al.. 2010. The polarisome is required for segregation and retrograde transport of protein aggregates. *Cell.* 140:257-267.
- Liu, L., T.A. Rando. 2011. Manifestations and mechanisms of stem cell aging. *J. Cell. Biol.* 193:257-66.
- López-Otín, C., M.A. Blasco, L. Partridge, M. Serrano, G. Kroemer. 2013. The Hallmarks of Aging. *Cell.* 153:1194-1217.
- Lu, W., M.O. Casanueva, A.P. Mahowald, et al.. 2012. Niche-associated activation of rac promotes the asymmetric division of Drosophila female germline stem cells. *PLoS Biol.* 10:e1001357.
- Ludwig, H., D. Khayat, G. Giaccone, T. Facon. 2005. Proteasome inhibition and its clinical prospects in the treatment of hematologic and solid malignancies. *Cancer.* 104:1794-1807.
- Luzio, J.P., P.R. Pryor, N.A. Bright. 2007. Lysosomes: fusion and function. *Nat. Rev. Mol. Cell Biol.* 8:622-632.
- Maeda, K., M. Takemura, M. Umemori, T. Adachi-Yamada. 2008. E-cadherin prolongs the moment for interaction between intestinal stem cell and its progenitor cell to ensure Notch signaling in adult Drosophila midgut. *Genes. Cells.* 13:1219-1227.
- Markesbery, W.R., M.A. Lovell. 1998. Four-hydroxynonenal, a product of lipid peroxidation, is increased in the brain in Alzheimer's disease. *Neurobiology of aging.* 19:33-6.
- Marques, C., P. Pereira, A. Taylor, et al.. 2004. Ubiquitin-dependent lysosomal degradation of the HNE-modified proteins in lens epithelial cells. *FASEB. J.* 18:1424-1426.
- McGrath, L.T., B.M. McGleenon, S. Brennan, et al.. 2001. Increased oxidative stress in Alzheimer's disease as assessed with 4-hydroxynonenal but not malondialdehyde. *QJM.* 94:485-90.

- McKearin, D., B. Ohlstein. 1995. A role for the *Drosophila* bag-of-marbles protein in the differentiation of cystoblasts from germline stem cells. *Development*. 121:2937-2947.
- Micchelli, C.A., N. Perrimon. 2006. Evidence that stem cells reside in the adult *Drosophila* midgut epithelium. *Nature*. 439:475-479.
- Moseley, J.B., B.L. Goode. 2006. The yeast actin cytoskeleton: from cellular function to biochemical mechanism. *Microbiol. Mol. Biol. Rev.* 70:605-45.
- Nawrocki, S.T., J.S. Carew, M.S. Pino, et al.. 2006. Aggresome disruption: a novel strategy to enhance bortezomib-induced apoptosis in pancreatic cancer cells. *Cancer Res.* 66:3773-81.
- Neumüller, R.A., J.A. Knoblich. 2009. Dividing cellular asymmetry: asymmetric cell division and its implications for stem cells and cancer. *Genes Dev.* 23:2675-99.
- O'brien, C.A., A. Kreso, P. Ryan, et al.. 2012. ID1 and ID3 Regulate the Self-Renewal Capacity of Human Colon Cancer-Initiating Cells through p21. *Cancer Cell*. 21:777-792.
- Ohlstein, B., A. Spradling. 2006. The adult *Drosophila* posterior midgut is maintained by pluripotent stem cells. *Nature*. 439:470-474.
- Ohlstein, B., A. Spradling. 2007. Multipotent *Drosophila* intestinal stem cells specify daughter cell fates by differential notch signaling. *Science*. 315:988-992.
- Okada, K., C. Wangpoengtrakul, T. Osawa, et al.. 1999. 4-Hydroxy-2-nonenal-mediated impairment of intracellular proteolysis during oxidative stress. Identification of proteasomes as target molecules. *J. Biol. Chem.* 274:23787-23793.
- Pan, L., S. Chen, C. Weng, et al.. 2007. Stem cell aging is controlled both intrinsically and extrinsically in the *Drosophila* ovary. *Cell Stem Cell*. 1:458-69.
- Parmentier, M.L., D. Woods, S. Greig, et al.. 2000. Rapsynoid/partner of inscuteable controls asymmetric division of larval neuroblasts in *Drosophila*. *J. Neurosci.* 20:, RC84.
- Pereira, G., T.U. Tanaka, K. Nasmyth, E. Schiebel. 2001. Modes of spindle pole body inheritance and segregation of the Bfa1p-Bub2p checkpoint protein complex. *EMBO J.* 20:6359-70.
- Phillips, J.P., S.D. Campbell, D. Michaud, M. Charbonneau, A.J. Hilliker. 1989. Null mutation of copper/zinc superoxide dismutase in *Drosophila* confers hypersensitivity to paraquat and reduced longevity. *Proc. Natl. Acad. Sci. USA.* 86:2761-5.
- Pine, S.R., B.M. Ryan, L. Varticovski, A.I. Robles, C.C. Harris. 2010. Microenvironmental modulation of asymmetric cell division in human lung cancer cells. *Proc. Natl. Acad. Sci. USA.* 107:2195-200.
- Ramdzan, Y.M., S. Polling, C.P.Z. Chia, et al.. 2012. Tracking protein aggregation and mislocalization in cells with flow cytometry. *Nat. Meth.* 9:467-470.
- Reed, S.I. 2003. Ratchets and clocks: the cell cycle, ubiquitylation and protein turnover. *Nat. Rev. Mol. Cell Biol.* 4:855-864.
- Reya, T., S.J. Morrison, M.F. Clarke, I.L. Weissman. 2001. Stem cells, cancer, and cancer stem cells. *Nature*. 414:105-11.

- Roesch, A., M. Fukunaga-Kalabis, E.C. Schmidt, et al.. 2010. A Temporarily Distinct Subpopulation of Slow-Cycling Melanoma Cells Is Required for Continuous Tumor Growth. *Cell*. 141:583-594.
- Rujano, M.A., F. Bosveld, F.A. Salomons, et al.. 2006. Polarised asymmetric inheritance of accumulated protein damage in higher eukaryotes. *PLoS Biol.* 4:, e417.
- Schriner, S.E. 2005. Extension of Murine Life Span by Overexpression of Catalase Targeted to Mitochondria. *Science*. 308:1909-1911.
- Sharma, S.V., D.Y. Lee, B. Li, et al.. 2010. A Chromatin-Mediated Reversible Drug-Tolerant State in Cancer Cell Subpopulations. *Cell*. 141:69-80.
- Shcheprova, Z., S. Baldi, S.B. Frei, et al.. 2008. A mechanism for asymmetric segregation of age during yeast budding. *Nature*. 454:728-734.
- Shellenbarger, D.L., J.D. Mohler. 1975. Temperature-sensitive mutations of the notch locus in *Drosophila melanogaster*. *Genetics*. 81:143-162.
- Shinin, V., B. Gayraud-Morel, D. Gomes, S. Tajbaksh. 2006. Asymmetric division and cosegregation of template DNA strands in adult muscle satellite cells. *Nat. Cell Biol.* 8:677-87.
- Siller, K.H., C. Cabernard, C.Q. Doe. 2006. The NuMA-related Mud protein binds Pins and regulates spindle orientation in *Drosophila* neuroblasts. *Nat. Cell Biol.* 8:594-600.
- Song, C.-Z., Z.-L. Bai, C.-C. Song, Q.-W. Wang. 2003. Aggregate formation of hepatitis B virus X protein affects cell cycle and apoptosis. *World J. Gastroenterol.* 9:1521-4.
- Song, X., C.-H. Zhu, C. Doan, T. Xie. 2002. Germline stem cells anchored by adherens junctions in the *Drosophila* ovary niches. *Science*. 296:1855-1857.
- Sousa-Nunes, R., L.L. Yee, A.P. Gould. 2011. Regulating neural proliferation in the *Drosophila* CNS. *Curr. Opin. Neurobiol.* 20:50-7.
- Todd, T.W., J. Lim. 2013. Aggregation formation in the polyglutamine diseases: Protection at a cost?. *Mol. Cells*. 2013:1-10.
- Tomaru, U., S. Takahashi, A. Ishizu, et al.. 2012. Decreased Proteasomal Activity Causes Age-Related Phenotypes and Promotes the Development of Metabolic Abnormalities. *Am. J. Pathol.* 180:963-972.
- Toroser, D., W.C. Orr, R.S. Sohal. 2007. Carbonylation of mitochondrial proteins in *Drosophila melanogaster* during aging. *Biochem. Biophys. Res. Commun.* 363:418-424.
- Tran, V., C. Lim, J. Xie, X. Chen. 2012. Asymmetric Division of *Drosophila* Male Germline Stem Cell Shows Asymmetric Histone Distribution. *Science*. 338:679-682.
- Vernace, V.A., T. Schmidt-Glenewinkel, M.E. Figueiredo-Pereira. 2007. Aging and regulated protein degradation: who has the UPPer hand? *Aging Cell*. 6:599-606.
- Waelter, S., A. Boeddrick, R. Lurz, et al. 2001. Accumulation of mutant huntingtin fragments in aggresome-like inclusion bodies as a result of insufficient protein degradation. *Mol. Biol. Cell*. 12:1393-407.
- Wang, X., J.-W. Tsai, J.H. Imai, et al.. 2009. Asymmetric centrosome inheritance maintains neural progenitors in the neocortex. *Nature*. 461:947-55.

- Wang, Y., A.B. Meriin, N. Zaarur, et al. 2009. Abnormal proteins can form aggresome in yeast: aggresome-targeting signals and components of the machinery. *FASEB. J.* 23:451-463.
- Westerink, R.H.S., A.G. Ewing. 2007. The PC12 cell as model for neurosecretion. *Acta Physiologica.* 192-273-285.
- Wong, C.M., L. Marcocci, L. Liu, Y.J. Suzuki. 2010. Cell signaling by protein carbonylation and decarbonylation. *Antioxid. Redox. Signal.* 12:393-404.
- Yadlapalli, S., Y. M. Yamashita. 2013. Chromosome-specific nonrandom sister chromatid segregation during stem-cell division. *Nature.* 498:251-254.
- Yamashita, Y.M., A.P. Mahowald, J.R. Perlin, M.T. Fuller. 2007. Asymmetric inheritance of mother versus daughter centrosome in stem cell division. *Science.* 315:518-21.
- Yanai, A., K. Huang, R. Kang., et al.. 2006. Palmitoylation of huntingtin by HIP14 is essential for its trafficking and function. *Nat. Neurosci.* 9:824-31.
- Yang, Z.J., C.E. Chee, S. Huang, F.A. Sinicrope. 2011. The Role of Autophagy in Cancer: Therapeutic Implications. *Mol. Cancer Ther.* 10:1533-1541.
- Zhou, C., B.D. Slaughter, J.R. Unruh, et al.. 2011. Motility and Segregation of Hsp104-Associated Protein Aggregates in Budding Yeast. *Cell.* 147:1186-1196.